Journal of Cosmology, Vol.26, No. 34, pp. 16131 – 16179

Gnomonic Scalar-Field Cosmology on Riemannian Manifolds: An Absorptive Framework Independent of Temporal Dynamics

Joseph E. Mullat *

Abstract. This work introduces a novel conceptual framework that integrates gnomonic visualization techniques with cosmological geometry. Specifically, we reinterpret the gnomonic holography of three-dimensional crystal structures onto a two-dimensional plane within the three-dimensional Riemannian Manifold metric, formulated following the Landau–Lifshitz approach. Within this framework, the surface of a four-dimensional hypermanifold (a 4D sphere) is heuristically and conjecturally interpreted as exhibiting topological features analogous to the ″inside–outside″ structure of a Klein bottle. This analogy is not intended as a strict topological identification, but rather as an illustrative conceptual device to motivate geometric intuition about global structure. This geometrical perspective provides a foundation for analyzing the mass–energy budget of the Universe as determined by the Planck mission. We examine the present mass–energy composition—including the relative contributions of visible (baryonic) matter and dark energy, identified here with the zero-point field (ZPF)—within a differential geometric setting. These components are ultimately represented through a gnomonic holography–based formulation of the Planck observational mass–energy budget.

Keywords: Differential Geometry; Cosmology; Planck's Mission; Gnomonic Holography; Riemannian Manifold; FLRW Metric

1. Introduction

Foundational research in cosmology and gravity has increasingly exposed the conceptual limits of standard spacetime models and their role in early-universe physics. George F. R. Ellis has highlighted the geometric assumptions and interpretive constraints of Riemannian cosmology (Ellis, 2014), motivating alternative formulations of gravity such as the geometric and topological approaches developed by Kirill Krasnov, which shift emphasis from metric variables to connections (Krasnov, 2011). In parallel, Carlo Rovelli has advanced relational and time-independent formulations of physics that challenge the notion of fundamental time (Rovelli, 2004; 2018). These conceptual developments are closely connected to the physics of early-universe phase transitions (Guth et al., 1980; Witten, 1984), which are tied to symmetry breaking at high energies and may have generated topological defects such as monopoles, cosmic strings, or domain walls (Kibble, 1980). Although such transitions occurred when the universe was opaque to light, their consequences—ranging from relic particles to primordial gravitational waves—may still leave observable imprints on the present universe.

About the author: Former docent at the Faculty of Economics, Tallinn Technical University, Estonia; Independent researcher. Docent is an Eastern European academic title equivalent to Associate Professor in the USA. Residence: Nygårdsvej, 10, 2s., Nr.13, 2100 Østerbro, Copenhagen, Denmark, E-Mail: mjoosep@gmail.com.

Recent findings from the James Webb Space Telescope have stimulated renewed discussion regarding aspects of cosmic evolution, particularly in the context of early galaxy formation. While the Big Bang model and the ΛCDM framework remain broadly successful in accounting for a wide range of observations, some Webb results have highlighted potential tensions—especially concerning the apparent abundance, mass, and maturity of high-redshift galaxies. These observations are subject to ongoing analysis and interpretation, and may reflect a combination of observational uncertainties, selection effects, and limitations in current modeling approaches. As such, rather than constituting a refutation of standard cosmology, these findings motivate further refinement of theoretical models and a careful reassessment of underlying assumptions.

The Standard Model of particle physics continues to provide an extremely successful description of known fundamental interactions, yet it is widely understood to be incomplete. Ongoing experimental efforts seek evidence of physics beyond the Standard Model, particularly in areas such as dark matter, neutrino masses, and the matter–antimatter asymmetry. To date, no definitive departures have been confirmed. While recent astronomical observations, including those from the James Webb Space Telescope, have raised questions about aspects of cosmological modeling, their implications for fundamental particle physics remain indirect and subject to interpretation. Consequently, claims of inconsistency should be regarded cautiously, pending further observational and theoretical clarification.

The latest discoveries from the James Webb Space Telescope suggest that our fundamental understanding of the universe, including the Standard Model's connection to cosmology, may be flawed. Observations have unveiled anomalies that cannot be explained within existing frameworks, casting doubt on long-held assumptions. The long-standing attempts to unify quantum mechanics and cosmic evolution into a ″theory of everything″ have yielded no promising results, and now even the foundational Lambda-CDM model and Big Bang predictions are being questioned. Without a clear theoretical direction, physicists are waiting for new experimental guidance, yet Webb's findings indicate that the expected ″New Physics″ might not be an extension of current models but rather a fundamental revision of our understanding of space, time, and the evolution of the universe. Cosmology, once a science of precision and vast datasets, now finds itself at a crossroads, requiring a radical rethinking of its core principles.

Amid these paradigm-shifting revelations from Webb, it is worth considering how earlier missions, such as the Planck Collaboration, can contribute to amendments in our cosmological models and offer a new perspective on the interpretation of past precision measurements.

The Planck Collaboration has already taken the detailed space-time structure into account. The European Planck satellite, launched in May 2009, completed its scheduled sky survey by November 2010. The mission continued until the liquid helium cooling the detectors was exhausted, with Helium-3 cooling for the high-frequency receiver running out in January 2012, and Helium-4 cooling for the low-frequency instrument following soon after. The instrument outperformed the American WMAP, launched in 2001, with better angular resolution, higher sensitivity, and a wider frequency range. Naturally, researchers eagerly awaited the announcement of Planck's cosmological results. Some astrophysical findings had already been published, revealing fascinating discoveries such as giant barriers of hot gas connecting galaxy clusters. A major cosmological data release was scheduled for 2013.

One of the most striking results concerns the cosmic recipe of the universe. Ordinary matter—protons, atomic nuclei, and electrons—accounts for only **5%** of the total space in the current universe. In addition to ordinary matter, the universe also contains relic neutrinos—about 300 neutrinos of all types per cubic centimeter. Their contribution to the total energy (mass) of the universe is small, given their low masses, and certainly does not exceed **3%**. However, the remaining **95%** of the universe's energy and matter has long been a mystery.

To introduce a scenario that emphasizes the geometric relationships among cosmological objects—relationships inferred from observational phenomena commonly attributed to dark matter—we adopt a revised terminology aimed at improving clarity and accessibility for a broader audience. In this context, what is traditionally referred to as dark matter is occasionally described as dark or hidden matter, a choice intended to ease comprehension without altering the underlying physical meaning. Likewise, dark energy is presented as a background energy field, or zero-point-field (ZPF), particularly when discussing the mathematical framework of our static-space scenario as formulated within the LL/Riemannian metric. These terminological and conceptual adjustments are designed to support a more intuitive understanding of the Universe's composition while facilitating discussion of its evolution and large-flow structure.

At first glance, the discussion may appear to be a straightforward presentation of familiar concepts. Indeed, numerous studies have addressed related topics, including those of W. Fischler and L. Susskind (1998) and Pablo Díaz et al. (2008). However, there isn't a standard or widely recognized result in the literature stating that the Riemannian metric admits (or is naturally associated with) a homomorphic gnomonic metric linking two established categories through a gnomonic holographic mapping of a four-dimensional hypermanifold onto a three-dimensional surface. This specific framework has not been previously explored. Furthermore, earlier studies have not employed the terminology of gnomonic holography in interpreting Figure 1.

Figure 1.

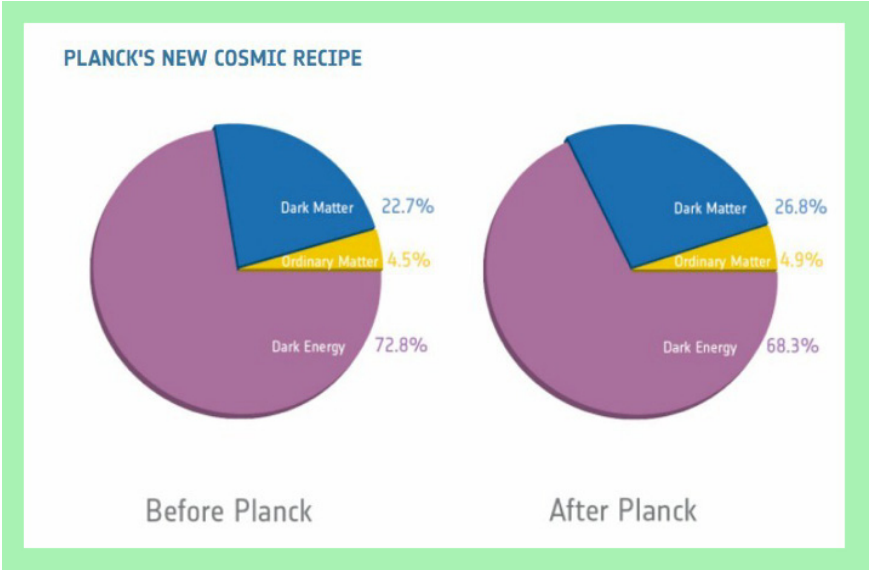

https://sci.esa.int/web/planck/-/51557-planck-new-cosmic-recipe.

The concept depicted in Figure 1 is much more profound than it might initially appear. Our analysis based on these data leads to the prediction that the Universe has already completed a full cycle of development, following a specific pattern derived from Le Sage's theory (18th century) in terms of the background energy field of gravitons (Danilatos, G., 2020, very carefully revises and corrects Le Sage-type gravity theory and the graviton absorption coefficient κ: see also Matthew R. Edwards, 2002).

Regarding the Figure 1, we read: "*Planck's high-precision cosmic microwave background map has allowed scientists to extract the most refined values yet of the Universe's ingredients. Normal matter that makes up stars and galaxies contributes just* ***4.93%*** *of the Universe's mass/energy inventory. Dark or hidden matter (quantum, jm.), which is detected indirectly by its graviton influence on nearby matter, occupies* ***26.40%****, while dark energy, a mysterious force thought to be responsible for accelerating the space capture of the Universe, accounts for* ***68.47%***", accessed online 26/07/2022.

If we consider perspectives—such as the alternative geometric interpretation of Big Bang model and the questionable predictions of the SM regarding the inflationary phase—the Le Sage's coefficient κ during the so-called primary inflation, as determined by the LL/Riemannian metric framework developed here, the κ must be estimated to be around $\infty \approx 10^{50}$. However, contemporary insights and empirical data, particularly the Planck cosmic recipe, indicate that the present-day background energy absorption coefficient κ' is approximately 0.125046486 (cf. Mullat, 2022).

As the universe continues expanding at a constant acceleration, our speculative model suggests that it will eventually reach a state of thermal and dynamic exhaustion—its ultimate ″death″—once the average density of energy absorbtion coefficient κ of the hypothetical ether (interpreted here as dark energy or the background gravitational field) falls to a critical threshold of $\kappa^{\bullet}$. At that point, the baryonic matter of the universe will remain intact but will be shrouded in darkness (with all visible light sources having vanished), occupying $\approx \frac{1}{3}$ of the total volume of the 3D Euclidian projection $\mathscr{E}^3$ of the 4D supermanifold $\Re^4$ surface. The remaining $\approx \frac{2}{3}$ of the space will be filled by traditionally identified as dark or hidden (surrounding matter). Meanwhile, the background energy field (ZPF) as mentioned earlier, will be completely depleted. As a consequence, Le Sage's pushing gravity forces should also disappear.

1.1. On the Replacement of Temporal Dynamics

Cosmology is mostly the study of how any valid model must enable predictions of the Universe scale factor $a(t)$ under different physical assumptions. Predictions underlie the success of classical mechanics and Einstein's general theory of relativity, particularly in explaining anomalies such as Mercury's orbital motion. In such frameworks, time t is an essential parameter.

By contrast, the present approach does not rely on time in the conventional sense. Rather than tracking motion, its objective is to predict the composition of the Universe—specifically its mass–energy distribution—near the Big Bang and in its terminal phase. This is formulated within a speculative framework in which potential energy is absorbed from a quantum vacuum or a hypothetical dark energy field.

In this model, dark ρ_c and visible matter ρ_b are represented as volumetric structures with radii $\rho_c = 0.670227254$ and $\rho_b = 3.061982489$, respectively, derived through a process termed *gnomonic holography*. Since absolute scales are unknown, the analysis proceeds using normalized relative quantities, expressed through percentage changes and volume variations within a so called κ-flow framework: $\kappa \equiv \kappa(\rho)$.

Planck-scale considerations indicate a substantial excess of dark $\Omega_c \approx 26.40\%$ over visible matter $\Omega_b \approx 4.93\%$, motivating the parametrization based on ρ radii. This yields a present absorption coefficient $\kappa' = \kappa(\rho_b)$, $\kappa' = 0.125046486$. The parameter κ is not treated as time-dependent, but as an interval-flow parameter representing successive phases of energy absorption. It describes a transition from an initial gravitational field to a mixed matter state, during which gravitational entropy decreases while mixture entropy increases.

As a result, the Universe becomes progressively more transparent to energy absorption. Thus, κ serves as an ordering parameter analogous to time, enabling consistent—though hypothetical—predictions without invoking explicit temporal evolution.

The model assumes that matter emerges through a phase transition of a primordial energy field. This is expressed through a normalized relation linking density variation, curvature scale, and κ, where the term $2 \cdot \pi^2 \cdot \Omega(\rho)$ represents the 3D volume of the Universe with gnomonic radius ρ instead of $a(t)$ scale factor. In this way, κ is embedded directly into the coupling between geometry and energy distribution at the point of emergence.

As κ decreases monotonically, total entropy increases. Higher κ corresponds to lower-entropy, gravitationally bound configurations, whereas lower κ corresponds to higher-entropy, weakly constrained mixed states. The evolution proceeds from an initial state dominated by gravitational potential, through a mixed present state $\Omega_\Lambda \approx 68.47\%$, toward a terminal configuration where vacuum energy $\Omega_\Lambda \to 0$. In this limit, mixture entropy dominates, ensuring a net increase in total entropy.

The absence of time may seem to preclude any meaningful notion of evolution. However, within this framework, change is governed instead by energy absorption from a primordial field, formalized as the κ-flow.

The flow κ is not continuous, but rather an ordered set of discrete values, each corresponding to a distinct absorption state. Its structure is purely relational: only the ordering of states, not requiring continuity or metric distance, makes sense; κ can be viewed as a function of the size of the universe, potentially expressed through the proposed trinity of nonlinear equations as a dynamical system that encodes both predictive and interpretative aspects of cosmic evolution.

Values of κ associated with conditions near the initial singularity dominant in magnitude, while values decrease toward a terminal state $\kappa^\bullet \approx 0.087273587$ as the Universe approaches thermal equilibrium. Within this framework, the geometry of the Universe is described by a parameter ρ, representing generalized distance in the cosmic manifold. In the absence of time, standard kinematics quantities such as velocity and acceleration lose their meaning. However, discrete analogs of derivatives can be introduced to evaluate transitions between states.

In fact, calibrating the current state of the universe using empirical data (e.g., Planck observations), a k-flow reference point k' can be established on the κ-scale. Past and future states are then interpreted relative to this reference within the flow.

In summary, although conventional temporal dynamics are absent, the model retains predictive and explanatory power through its geometric formulation. Cosmic evolution is described not as a function of time, but as an ordered progression through discrete states of energy absorption.

1.2. Early-Universe Phase Transitions and Their Cosmological Signatures

- A cosmological phase transition refers to a fundamental change in the state of matter throughout the universe, driven by the extreme conditions of the early cosmos. Theoretical models historically inspired by the success of the Big Bang framework suggested that such transitions occurred when the universe was much hotter and denser than today (Guth et al., 1980; Witten, 1984). However, recent observations from the James Webb Space Telescope (JWST) have challenged aspects of the Big Bang model, prompting reconsideration of early-universe cosmology. Despite this, the concept of phase transitions remains a key topic in modern theoretical physics, as they are deeply connected to highenergy symmetry breaking and the evolution of fundamental forces.
- These transitions could have led to the formation of topological defects such as magnetic monopoles, cosmic strings, or domain walls, depending on the underlying particle physics; cf. Guth. Additionally, they may have played a crucial role in cosmic inflation, baryogenesis, and the generation of primordial gravitational waves. Even though these events happened in the first moments of cosmic history, when the universe was opaque to light, their potential imprints-such as gravitational waves or relic particle abundances-might still be detectable today, offering valuable insights into the fundamental forces that shaped the cosmos (Kibble, 1980).

1.3. Rethinking the Singularity of the Big Bang

- The Newtonian potential energy field scalar indicator

$$-G\cdot\frac{m}{\rho}$$

was used. The critical transition is hypothesized to occur when the gravitational potential energy at the initial slice, characterized by a radius $\rho_0^0 \approx 0$, gives rise to the Universe's center and satisfies the condition

$$-\mu_\kappa \cdot \frac{M_0}{\rho_0^0} \le -\Delta .$$

Here, μ_κ, following Danilatos (2020), denotes the gravitational constant coupling parameter, while Δ, represents a dark-energy phase-transition threshold associated with matter M_0 formation; Within the framework, cf. the Brans–Dicke theory (1961), the gravitational constant **G** is generalized to a scalar field, thereby permitting spatio-temporal variation. The above condition, singular at $\rho_0^0 \approx 0$, may be reformulated as

$$-\mu_\kappa \cdot M_0 + \Delta \cdot \rho_0^0 \le 0$$

eliminating the singularity. Under this interpretation, the initial dark-energy phase transition that generated the Universe—commonly identified with the Big Bang—is not an explosion, but rather a rapid conversion of an underlying energy field into matter.

1.4. A Proposed Formulation of Cosmological Genesis

• Within the framework of *Pushing Gravity*, we introduce an absorption parameter κ. The admissible absorption values κ lie within an interval approximately given by

$$(\kappa_\infty > ... > \kappa' = 0.125046486. > ... > \kappa^\bullet \approx 0.087273587]$$

• The governing constraint is defined by

$$\Gamma(\rho, \mu, \lambda, \Delta) = -\mu_\kappa \cdot V(\mathcal{S}_\rho^3) \cdot \mu + \Delta \cdot \rho^\lambda \le 0,$$

that refers more concisely to the latter in form (5), as Γ **-equation** (for "="), or (for "<")—the Γ **-condition**. Here, λ and Δ are intrinsic constants, while μ **represents** the average density of matter inside a 3D gnomonic holographic sphere $\mathcal{S}_\rho^3$ of radius ρ. In this context, $\mathcal{S}_\rho^3$ corresponds to the volume $V(\mathcal{S}_\rho^3)$ of the three-sphere $\mathcal{S}_\rho^3$. By substitution

$$\mu_\kappa = \frac{\kappa}{\mu}$$

—which was inspired by analogy with the Beer–Lambert law of absorption, and also pointed out by Danilatos (2020)—the Γ -condition (or equation) can be simplified to the form

$$\Gamma(\rho, \kappa, \lambda, \Delta) = -\kappa \cdot V(S_\rho^3) + \Delta \cdot \rho^\lambda \le 0,$$

that removes the explicit dependence on the average density parameter μ. The Γ **-condition** reveals a defining sequence (Mullat, 1971a, or particularly in the $\mathbf{M}^+$ Monotone system,1976b),

$$\Gamma(\rho_i^j, \kappa_i, \lambda, \Delta) \approx 0 < < \rho_0^0 < \rho_0^1 < \rho_0^2, ... \rho_i^j < \rho_i^{j+1} ...$$

• This sequence may be interpreted as a **cosmological genesis process**, driven by successive absorptions $\kappa_i^j \ge \kappa_i^{j+1} \ge \kappa_i^{j+2} > ... > \kappa_i ... > \kappa_{i+1} ... > \kappa_{i+2} ...$ of the Universe's zero-point-field (ZPF) energy. The sequences ρ_i^j converge asymptotically such that

$$\lim_{j \to \infty} \Gamma(\rho_i^j, \kappa_i, ...) \to \Gamma(\rho_i, \kappa_i, ...) = 0, \Gamma(\rho_{i+1}, \kappa_{i+1}, ...) = 0, ...$$

indicating stabilization toward the Γ **-equation** (5) state.

1.5. Compatibility with the Observed Composition of the Universe

- In physics, the measurement of any phenomenon—or, more fundamentally, the definition of a reference flow—requires the introduction of an appropriate standard. This typically involves the construction of a measuring instrument, such as a clock, followed by its calibration to ensure predictive consistency with empirical observations. For instance, a clock must be calibrated so that its readings correspond to terrestrial time, while a thermometer is calibrated by fixing its zero point according to experimental benchmarks. A standard example is the assignment of 0 °C to the freezing point of water, or −17.8 °F to the freezing point of a supersaturated saline solution.
- In cosmology, however, the situation is fundamentally different. Our primary observational instrument is the telescope, and the question becomes not how to construct a device, but what physical quantity we choose to measure. In the present framework, this issue is further complicated by the absence of time as a fundamental parameter, which might suggest that predictive statements are no longer possible. Nevertheless, predictions can still be formulated by introducing an alternative reference flow—namely, an absorption flow defined through the vacuum energy field absorption coefficient, denoted by κ. Within this approach, observational input is provided by results from the Planck mission, that constrains the present-day matter–energy composition of the Universe.
- To operationalize this approach, we propose using observational results from the Planck mission to determine the present composition of matter in the Universe. The central tool in this analysis is the Γ-equation (5), which, once properly calibrated, is expected to reproduce the Planck solution. By setting $\lambda = 0.843370586$ and $\Delta = 0.913196709$, and imposing the condition $\Gamma(\rho, \kappa, \lambda, \Delta)$, we particularly obtain $\kappa' = 0.125046486$. This value can thus be encompassed as the present-day absorption coefficient on the κ-flow.
- Within this framework, κ evolves systematically from higher to lower values during the formation of the Universe. Consequently, deviations from the present value $\kappa' = 0.125046486$—either toward larger or smaller values—correspond to different states of the energy–matter composition. In this way, movement along the κ-flow provides a basis for predicting the past and future balance of energy and matter in the Universe.
- Accordingly, the present construction should be understood as a dynamically constrained system in which geometry, holography, and cosmological 2018 observation data are mutually synchronized through the evolution of matter density as the Planck parameters $\Omega_c \approx 0.2640$, $\Omega_\Lambda \approx 0.6847$, $\Omega_b \approx 0.0493$

(Aghanim et al, 2020; arXiv: 1807.06209), corresponding respectively to the cold-dark-matter, dark-energy, and baryonic density fractions of the contemporary Universe — may therefore be incorporated into some dynamical mechnism in the form of nonlinear dynamical system $F(\rho, \kappa, \lambda, \Delta)$ of type (6) leading to a synchronized configuration of fixed points while preserving the underlying geometric–holographic principles of the model. There do not exists net positive solutions of Γ-equation (5) for $\kappa < \kappa^{\bullet} = 0.087273587$. The *"death or terminal phase"* of the Universe is assigned to $\kappa^{\bullet}$ (only for complex).

1.6. The Dark Matter, the Klein Bottle Conjecture, and the Geometry of Space

In astrophysics and cosmology, the verification of hypotheses and speculative propositions cannot rely on controlled laboratory experiments, as is common in terrestrial physics. Instead, such verification depends critically on the development and testing of mathematical models grounded in observational data and guided by physically motivated intuition. Within this context, it is important to distinguish clearly between empirically supported frameworks and heuristic or conjectural extensions.

The existence of dark matter is generally framed as an inference from gravitational phenomena rather than a directly observed component. Key evidence includes the anomalous dynamics of galaxy clusters, first identified by Fritz Zwicky (1933), and the flat rotation curves of spiral galaxies, systematically studied by Vera Rubin and collaborators (1970–1980). While these observations strongly support the presence of additional gravitating mass, the underlying nature of dark matter remains unresolved.

Motivated by these considerations, we outline here a heuristic and conjectural geometric interpretation of the dark matter problem. This framework is not presented as a rigorously established model, but rather as an exploratory construction intended to illustrate how topological features of space might, in principle, contribute to the observed phenomenology.

Specifically, we consider a conjectural scenario in which the global topology of the universe exhibits features analogous to a Klein bottle. In this picture, visible (baryonic) matter and dark matter are not necessarily separate substances in the conventional sense, but may instead correspond to regions that are topologically connected yet locally inaccessible within three-dimensional space. Any such interpretation should be regarded as speculative and illustrative rather than derived from first principles.

A similar heuristic mapping can be invoked when considering cosmological coordinates. Under certain transformations (e.g., gnomonic-type mappings), Riemannian regions that appear widely separated in standard coordinates may

correspond to identical or related parameter values in an alternative representation. While such mappings can be mathematically well-defined, their physical interpretation in terms of inaccessible sectors of the universe remains conjectural and requires further justification.

Within this speculative framework, one may imagine that gravitational effects could, in principal, probe aspects of the global geometry that are not directly accessible through local interactions. However, the extension of this idea to a concrete physical mechanism—such as embedding in a higher-dimensional manifold or invoking a zero-point energy field—remains hypothetical and is not currently supported by direct empirical evidence.

Accordingly, the apparent invisibility of dark matter is here interpreted, at a conjectural level, as a possible manifestation of geometric and topological structure rather than solely as a consequence of unknown particle properties. This interpretation should be regarded as a conceptual proposal that complements, but does not replace, existing particle-based and astrophysical models.

To clarify this idea, and drawing more generally on geometric perspectives (Galloway et al., 2022; Putz & Ori, 2026), consider a thought experiment involving a Klein bottle embedded in a higher-dimensional manifold $\mathcal{R}^4$. Two observers — one (Ω_b) situated on what may be described as an "outer" region and another (Ω_c) on a "hidden" region — inhabit the same continuous surface but are unable to interact through local, intrinsic pathways. This construction is intended purely as an analogy: it does not reflect a specific claim in the cited works, but rather illustrates how geometric structure alone may allow global connectedness to coexist with local inaccessibility.

This scenario arises when describing the observable universe from the perspective of an observer located at the origin, $\rho = 0$. The Riemannian domain accessible to observation can be divided into two regions,

$$0 \le \rho < 1 \text{ and } 1 \le \rho < \infty ,$$

which appear disconnected despite being related through a Klein bottle coordinate mapping. Such a mapping in line with gnomonic holography is defined by

$$r(\rho) = \frac{2 \cdot \rho}{1 + \rho^2},$$

under which the coordinate r increases from $r=0$ to $r=1$ as ρ runs from 0 to 1, and then decreases from $r=1$ back toward $r=0$ as ρ extends from 1 to infinity. As a consequence, two observers located at widely separated positions ρ' and ρ'', with

$$\rho' << \rho'',$$

may nevertheless share the same gnomonic coordinate, satisfying $r(\rho')=r(\rho'')$. Despite this apparent coincidence, they remain deprived of interaction opportunities, much like two individuals on the bottle—one inside and one outside—for whom the condition

$$r'=r''$$

does not guarantee interaction. Although no interaction opportunities exist within three-dimensional space $\mathcal{E}^3$, interaction becomes possible through higher-dimensional embedding. Indeed, when the bottle is embedded in manifold $\mathcal{R}^4$, the additional dimension allows the ″neck″ of the bottle to pass through itself without self-intersection.

By analogy, observers in our universe cannot access dark matter through any known local interaction channels within $\mathcal{E}^3$, yet they can infer its existence through gravitational effects arising in a four-dimensional space $\mathcal{R}^4$. In this framework, the additional coordinate may be represented as a line connecting the poles of a four-sphere, from the North Pole

$$N_p=(0,0,0,+1)$$

to the South Pole

$$S_p=(0,0,0,-1).$$

Dark matter, while hidden along this fourth coordinate, nevertheless curves spacetime and influences the motion of visible/baryonic matter.

Thus, the absence of direct detection of (DM) dark matter need not be interpreted as evidence of its nonexistence, but rather as a manifestation of the geometric and topological structure of the universe. In this framework, visible (baryonic or VM) matter is confined to the ″outside″ of the bottle, fully embedded within the familiar three-dimensional Riemannian manifold accessible to electromagnetic and nuclear interactions. Dark matter, by contrast, occupies a topologically distinct region—effectively ″inside″ the bottle— that is globally connected yet locally inaccessible to observers confined to 3D Euclidian space ($\mathcal{E}^3$).

Observers moving on different regions of the bottle provide an instructive conjecture. Although the ″inside″ and ″outside″ are part of a single, continuous global geometry, observers constrained to one region cannot directly interact with those on the other through local, non-gravitational means. No exchange of light or particles is possible; nevertheless, gravitational influence transcends this topological separation, allowing matter residing outside the observers' immediate dimensional domain to imprint itself dynamically.

In summary, the Klein bottle analogy and the associated higher-dimensional embedding should be understood as heuristic tools for thinking about the dark matter problem. They highlight the possibility that global topology and dimensional structure could play a role in shaping observable phenomena, but they do not, in their present form, constitute a predictive or empirically validated model.

1.7. Reading Guide

When reading the paper, it helps to classify statements into three layers:

Layer 1 — Established Foundations

These are well-supported:

- Differential geometry
- Riemannian manifolds
- FLRW cosmology
- Planck cosmic microwave background measurements
- Dark matter and dark energy as observational phenomena

Layer 2 — Legitimate Open Questions

These remain active areas of research:

- The particle nature of dark matter
- The origin of dark energy
- Quantum gravity
- The very earliest moments of the Universe
- The global topology of the Universe

Layer 3 — The Paper's Original Hypotheses

These are the author's proposed ideas:

- Eliminating time as a fundamental cosmological variable
- κ-flow replacing temporal evolution
- Gnomonic holography as a description of the Universe
- Dark matter as a topologically hidden region
- ZPF absorption driving cosmic evolution
- Le Sage–type absorptive gravity

1.7.1. Comparative Glossary: Standard Cosmology vs. Mullat's Gnomonic κ-Flow Framework

Term	Standard Physics / Cosmology	Mullat's Interpretation in This Paper
Big Bang	The early hot, dense state from which the observable Universe expanded; described by FLRW cosmology and supported by observations such as the cosmic microwave background and cosmic expansion.	Reinterpreted as a **phase transition** in which an underlying energy field converts into matter, rather than as a conventional temporal explosion.
Time (t)	A fundamental coordinate in relativity. Cosmological evolution is normally described by the scale factor **a(t)** changing with time.	Removed as a fundamental variable. The Universe is described by progression along a **κ-flow** of energy absorption states rather than through time.
Scale Factor a(t)	A function in FLRW cosmology describing how distances between cosmic objects evolve over time.	Replaced by a geometric gnomonic radius **ρ**, which represents states of the Universe within a projected manifold.
FLRW Metric	The standard mathematical description of a homogeneous and isotropic Universe in general relativity.	Treated as a Riemannian spatial slice that can be reformulated through gnomonic holographic geometry.
Riemannian Geometry	The mathematics of curved spaces using metrics, curvature, and manifolds. Essential to general relativity.	Used as the foundation for a gnomonic representation of a higher-dimensional cosmological structure.
Gnomonic Projection	A known geometric projection that maps points on a sphere to a plane using rays from a central point. Used in cartography and crystallography.	Generalized into "gnomonic holography," a proposed mapping between higher-dimensional cosmological manifolds and observable space.
Holography	In modern theoretical physics, usually refers to the holographic principle (e.g., information in a volume being represented on a boundary).	Used in a geometric sense as a projection or encoding of higher-dimensional structures into lower-dimensional space.
Dark Matter	A gravitationally inferred component of the Universe that does not interact electromagnetically. Its microscopic nature is unknown.	Speculatively interpreted as matter occupying a geometrically hidden region of a Klein-bottle-like higher-dimensional topology.
Dark Energy	A component responsible for the observed accelerated expansion of the Universe, represented in standard cosmology by the cosmological constant Λ or related models.	Identified with a zero-point background energy field (ZPF) that is gradually absorbed during cosmic evolution.

Term	Standard Physics / Cosmology	Mullat's Interpretation in This Paper
Zero-Point Field (ZPF)	A concept from quantum field theory describing vacuum fluctuations and minimum-energy states. Its relation to dark energy is a subject of ongoing theoretical investigation.	Treated as a cosmic energy reservoir that supplies the Universe through an absorption process governed by κ.
Absorption Coefficient κ	No standard cosmological parameter with this role exists.	A central new parameter describing the degree of energy absorption from the ZPF and ordering cosmic states.
κ-Flow	No direct equivalent in conventional cosmology.	The replacement for temporal evolution: an ordered sequence of absorption states from primordial conditions to a terminal equilibrium.
Entropy	A measure of the number of possible microscopic states; in cosmology it is related to thermodynamic and gravitational processes.	The model proposes a transition from a high-κ, low-entropy gravitational state toward a low-κ, high-entropy terminal state.
Planck Mission Data	High-precision observations of the cosmic microwave background used to determine cosmological parameters.	Used as calibration targets to synchronize the model's internal parameters so it reproduces the observed matter–energy proportions.
Cosmic Composition $(\Omega_b, \Omega_c, \Omega_\Lambda)$	The fractions of baryonic matter, cold dark matter, and dark energy in the standard cosmological model.	Treated as geometric volume fractions emerging from gnomonic projections and the κ-dependent dynamic system.
Klein Bottle	A non-orientable mathematical surface with no distinct inside or outside when embedded in four dimensions.	Used as a heuristic analogy to explain how visible and dark sectors might be globally connected yet locally inaccessible.
Higher Dimensions	Explored in some theories such as string theory, but not part of the standard ΛCDM model.	A four-dimensional manifold is used as the geometric background from which the observable Universe is projected.
Gravity	In general relativity, gravity arises from the curvature of spacetime caused by energy and momentum.	The paper explores ideas connected to Le Sage–type "pushing gravity" and energy absorption mechanisms as part of its speculative framework.
Prediction	A successful scientific theory predicts phenomena that can be independently tested.	The model aims to reproduce the Planck mass-energy distribution through geometric relations and κ-flow dynamics.

1.7.2. Roadmap

The structure of the paper is organized as follows.

Section 1 introduces the conceptual motivation for the work and situates it within current tensions in cosmology, particularly those arising from Planck mission results and recent James Webb Space Telescope observations. The section emphasizes the need for alternative geometric interpretations of cosmological data that do not rely fundamentally on temporal dynamics.

Subsection 1.6 develops the geometric **interpretation of dark matter** using the Klein bottle conjecture. This discussion explains the apparent invisibility of dark matter as a consequence of topological separation within a higher-dimensional embedding space, rather than as a failure of particle detection. The Klein bottle is employed strictly as a geometric visualization tool to illustrate ″inside–outside″ duality in gnomonic coordinates.

Section 2 (Preliminaries) establishes the methodological and conceptual foundations of the analysis. Occam's Razor is adopted as a guiding principle, motivating the deliberate elimination of explicit time dependence. Background material from crystallography, differential geometry, and the Riemannian manifold spatial-slice formalism in the Landau–Lifshitz framework is reviewed.

Section 3 introduces gnomonic holography in its simplest setting by mapping the two-dimensional spherical surface $\mathcal{S}^2$ onto the Euclidean plane $\mathcal{E}^2$. This section serves as a pedagogical preparation for the higher-dimensional constructions that follow.

Section 4 generalizes the gnomonic holography to a four-dimensional hypermanifold $\mathcal{R}^4$, mapping its three-dimensional surface $\mathcal{S}^3$ onto Euclidean space $\mathcal{E}^3$. The gnomonic Landau–Lifshitz (LL/Riemannian) slice is derived explicitly, and cosmological volumes are computed in holography coordinates. This section provides the geometric basis for interpreting the Planck cosmic mass–energy budget.

Section 5 applies the gnomonic LL/Riemannian framework to the observed composition of the Universe. By redefining velocity (8) and acceleration (9) in purely geometric terms—expressed as percentage change per megaparsec rather than as time derivatives—the Planck 2018 cosmic recipe emerges as a consistency condition of the model. The agreement with observational data is emphasized as a validation of the geometric framework rather than as a prediction.

Section 6 (Concluding Remarks) summarizes the main results and highlights the model-dependence of cosmological mass–energy budgets. It argues that the gnomonic LL/Riemannian approach, combined with monotonic systems theory, provides a flexible alternative to standard ΛCDM interpretations and is potentially better aligned with recent JWST observations.

Taken together, Sections 2–6 demonstrate that the Universe's observed mass–energy budget, can be coherently interpreted as consequences of gnomonic geometry applied to Riemannian slices—without reliance on fundamental time or supplementary dynamical postulates.

2. Preliminaries

We will work based on Occam's Razor—a principle with roots tracing back to Aristotle. It is a foundational methodological guideline of parsimony, which advises: *"Do not multiply entities beyond necessity" or "Do not introduce new entities unless absolutely required. "* This heuristic serves as a guiding framework in both philosophy and science, favoring simplicity over complexity in the construction of theoretical models. Although not a strict rule, Occam's Razor promotes the elimination of superfluous assumptions and discourages unnecessarily elaborate constructs unless there is compelling evidence for their inclusion. (Accessed online, 05.04.2025, https://www.britannica.com/topic/Occams-razor)

We reaffirmed our commitment to this principle by treating time as irrelevant in the scenario that follows, while simultaneously describing a sequence of k-expanding configurations of Universe and introducing a κ-flow—a form of parametric temperature, whether one chooses to call it that or not, analogous to a time flow.

To us, reality appears as a multitude of faces, each reflecting distinct speculations—speculations that can be true and false at the same time. Our model, as presented, does not lack falsifiability or physical foundations. On the contrary, we provide derivations that are directly connected to observable phenomena. The model's predictive power lies in its unconventional approach to temporal dynamics: rather than relying on the conventional time parameter, it derives the energy absorption coefficient as the key to scaling the Universe's composition. All of these ″alleged predictions″ are framed within the holography of Riemannian slice geometry.

In our context, this principle informs a deliberate attempt to reduce theoretical overhead. Specifically, we are choosing to abandon the use of high-rank tensors, explicit time coordinates, and external physical laws such as gravity, which, while potentially relevant in certain broader frameworks, are not strictly necessary for the conceptual scope of our analysis. Instead, we focus exclusively on the standard quadratic forms of differential geometry, which provide a rich but parsimonious mathematical language to describe curvature, structure, and Riemannian relationships within our system. These quadratic forms—often manifesting as metrics on smooth manifolds—allow us to capture essential geometric and topological features without resorting to the full machinery of more complex physical theories.

By adhering to this minimalist approach, we aim to clarify the intrinsic geometric structure of the problem at hand, stripping away potentially obfuscating layers and emphasizing only those mathematical tools that are essential for a precise and elegant description. This aligns with the deeper scientific tradition of seeking conceptual economy—a hallmark of theories that not only describe reality effectively but do so with elegance and explanatory power.

2.1. Gnomonic crystallography

In crystallography, various holographys are used to create images of crystals under study, allowing for detailed visualization of their symmetry elements, lattice orientation, and limiting faces. These holographys are fundamental tools for interpreting the geometric and symmetrical properties of crystalline structures. One of the most commonly used methods is the gnomo-stereographic holography, which combines aspects of both gnomonic and crystallographic techniques.

The gnomon is a scientific instrument historically used to measure the position of the sun by casting a shadow on a horizontal plane. This principle is adapted in stereography to represent directions and orientations in three-dimensional space. In constructing a crystal holography, the crystal is conceptually placed at the center of a spherical surface. Its faces and edges are extended outward until they intersect with this imaginary sphere. In a gnomonic holography, these intersections are then golographed onto a two-dimensional plane, typically along lines extending from a point on the sphere (often the North Pole) to a holography plane tangent to the South Pole. In this method, the faces of the crystal appear as circular arcs, and the edges appear as points, capturing angular relationships and symmetries accurately without significant distortion.

However, for a more intuitive and visual understanding of the crystal's geometry and symmetry relationships, crystallographers often use gnomonic holography. This method differs in that it projects the normals (perpendiculars) to the crystal faces, rather than the faces themselves. Consequently, the orientations of these face normals are mapped onto the surface of the sphere and then golographed onto a plane. In this approach, the faces are represented as points, corresponding to their orientation, while edges become arcs that connect these points, representing angular relationships between adjacent faces. This form of holography is particularly useful for analyzing the angular symmetry, pole figures, and the distribution of gnomonic directions in space.

Crystallography, at its core, is the study of the atomic arrangement within crystals and the symmetrical patterns they form. These holographys serve as essential visualization tools in this science, enabling crystallographers to interpret complex three-dimensional structures and their symmetries in a two-dimensional format, facilitating analysis, classification, and prediction of crystal behavior and properties.

2.2. Riemannian Manifold Slice: A Universe in Symmetry

In the grand narrative of modern cosmology, there exists a powerful idea—simple in symmetry, profound in implication—that describes the very shape and fate of the universe. This idea is encoded in a geometric construct known as the Riemannian metric, a mathematical expression that captures the large-distance structure of space and time.

The story begins in the early 20th century, as physicists and mathematicians grappled with the implications of Einstein's general theory of relativity. Einstein had revolutionized our understanding of gravity, recasting it not as a force but as a curvature of spacetime itself. But while his equations were majestic, they were also immensely complex. To extract cosmic-distance predictions, simplifications were needed—assumptions about the universe as a whole.

Enter Alexander Friedmann, a Russian physicist and mathematician. In 1922, Friedmann took Einstein's equations and boldly applied them to an idealized universe—one that is homogeneous (the same in every location) and isotropic (the same in every direction). These assumptions, radical in their elegance, allowed him to derive solutions that described not a static cosmos, as Einstein had hoped, but a dynamic one—expanding or contracting, driven by its own matter and energy content.

Shortly after, Georges Lemaître, a Belgian priest and physicist, independently arrived at a similar solution. He proposed what would later be called the ″primeval atom″ or the ″Big Bang″ theory. Lemaître wasn't just echoing Friedmann's math—he went further, connecting the expanding universe to astronomical observations, such as the redshift of galaxies. This wasn't just a speculative model; it was a model grounded in the observable cosmos.

Years later, in the United States and the United Kingdom, Howard P. Robertson and Arthur Geoffrey Walker formalized and extended this framework, expressing the metric in a form that could accommodate different possible curvatures of space: positive, negative, or flat. Their collective work led to the formulation of what we now call the FLRW metric—a mathematical description of a path-connected universe that, while continuous and traversable, is not necessarily simply connected, meaning it might possess topological quirks such as holes or loops.

At its spacial slice, the FLRW assumes that the universe, on the largest distances, can be treated as smooth and symmetric Riemannian metric. With these geometric assumptions, the metric reduces Einstein's field equations to a more manageable form, resulting in the Friedmann equations—differential equations that describe how the scale factor $a(t)$ of the universe evolves over time.

These equations are the backbone of the conceptual framework of Cosmology, often called the Lambda-CDM model (where Lambda represents dark energy and CDM stands for cold dark matter). While this model has successfully explained a wide array of cosmological observations—such as the cosmic microwave background, the formation of large-distance structures, and the accelerating expansion of the universe—recent discoveries from the James Webb Space Telescope have led some astronomers to question its completeness or validity.

Today, the FLRW metric is more than a mathematical convenience—it is a gateway to understanding our universe's past, present, and future. It connects theoretical physics to observational astronomy, and the insights of four scientists from diverse backgrounds and nations now stand together at the foundation of cosmological science.

Whether referred to FLRW or Riemannian, the metric is a testament to the power of symmetry, geometry, and international collaboration in unraveling the deepest mysteries of the cosmos. It teaches us that even the most abstract equations can reveal truths about the stars, galaxies, and the very nature of space and time itself.

2.3. Synthesis of Crystallography and Riemannian Slice

First, we describe the observational limitations and the inferred large-distance homogeneity and isotropy of the Universe. The finite speed of light imposes an observational horizon, such that we perceive distant cosmic structures not as they are now, but as they were when their light first began traveling toward us. Despite this, the large-distance structure of the observable Universe, as supported by cosmic microwave background measurements and galaxy surveys, appears statistically homogeneous (uniform across space) and isotropic (uniform in all directions). These empirical findings align with the Copernican Principle, which asserts that no location in the Universe is privileged—a conceptual extension of Copernicus's original insight that the Earth does not occupy a central, special position.

This foundational principle provides the logical basis for modeling the Universe with the FLRW Manifold metric, a solution to Einstein's field equations under the assumption of large-distance symmetry. Among the clearest formulations of this approach is found in ″The Classical Theory of Fields″ by Landau and Lifshitz, 3rd Revised English Edition, 1971, particularly Chapter 12, paragraph 107, expression 107.7. There, a closed, isotropic model is presented, in which the Universe possesses constant positive curvature—a geometric framework that directly yields the Riemannian metric in its closed-form expression.

What we propose here is a novel synthesis: the Riemannian (the spacial sclice of the FLRW) metric, interpreted through the lens of Landau and Lifshitz's field theory, can be understood as a gnomonic holography of cosmological geometry, much like the crystallographic and gnomo-stereographic methods used in crystallography to represent complex three-dimensional forms on a two-dimensional surface. In crystallography, these holographs are employed to encode the symmetrical properties and orientations of crystal structures in an idealized, often spherical space. Analogously, the Riemannian metric can be viewed as a mapping of the Universe's large-distance structure, gologaphed from a higher-dimensional manifold governed by its curvature and symmetry properties onto a coordinate framework suitable for cosmological analysis.

Just as gnomonic holography reveal the symmetry operations and constraints inherent in crystal lattices, the Riemannian metric—particularly in its closed form—captures the curvature-induced topology and symmetry constraints of the Universe as a manifold. The Landau–Lifshitz formulation, built within the rigorous language of differential geometry and classical field theory, provides the mathematical apparatus for interpreting the metric tensor as a field over a curved spacetime manifold, akin to how crystallographers interpret the lattice vectors and face normals as gologaphed features on a spherical representation.

Thus, in this interpretation, the Copernican homogeneity and isotropy correspond to the space-group symmetries in stereography; the Riemannian geometry corresponds to the unit cell or Bravais Lattice in momentum space; and the LL cosmological metric acts as the mapping function—a field-theoretic, differential-geometric analog to the gnomonic holographys of crystallography. The Riemannian manifold is, therefore, not just a mathematical abstraction but a cosmic lattice, gologaphed into observable coordinates through the symmetry conditions dictated by general relativity.

In this framework, cosmology borrows tools from the geometry of matter, transforming the Universe itself into a macro-crystal of spacetime—a coherent, self-similar structure that obeys symmetry principles at all observable distances. The connection between gnomonic methods and relativistic cosmology, when interpreted through Landau and Lifshitz's field-theoretic formulation, opens the door to new analogies and mathematical tools for understanding the geometry of the Universe—not merely as a solution space to Einstein's equations, but as a structured holography, shaped by symmetry, topology, and the fields that bind them.

Landau and Lifshitz incorporate these principles into their cosmological framework. They assume that, at a sufficiently large distance, the Universe obeys these symmetries, naturally leading to Reiemannian metric expressed in terms of a radial coordinate r that measures distances on a three-dimensional sphere $\mathcal{S}^3$:

$$dl^3 = \left(1 - \frac{r^2}{a^2}\right)^{-1} \cdot dr^2 + r^2 \cdot \left(\sin^2(\theta) \cdot d\varphi^2 + d\theta^2\right) \qquad (1)$$

This metric explicitly reflects the assumed homogeneity and isotropy, ensuring that all points and directions in space are equivalent. It provides a geometric foundation for modeling a closed universe, consistent with the fundamental assumptions of cosmology and depends on the curvature radius a, where the r can vary from 0 to a, and where φ and θ are in the intervals $[0 \le \varphi \le 2\pi]$ and $[0 \le \theta \le \pi]$. It turns out that the quadratic metric (1) can be considered as a gnomonic holography of the surface $\mathcal{S}^3$ of the four-dimensional hypermanifold $\mathcal{R}^4$ onto the flat Euclidean space $\mathcal{E}^3$. Indeed, the substitution

$$r = \frac{r_l}{1 + \frac{r_l^2}{4 \cdot a}} \text{ for } 0 \le r_l \le a \text{ lead to}$$

$$dl^3 = \left(1 + \frac{r_l^2}{4 \cdot a^2}\right)^{-2} \cdot \left(dr_l^2 + r_l^2 \cdot d\theta^2 + r_l^2 \cdot \sin^2\theta \cdot d\varphi^2\right). \qquad (2)$$

According to LL's intention, at every point of a 3-dimensional manifold $\mathcal{S}^3$ it would locally be Euclidean but curved for far away distances. By making the substitution $r_l = 2 \cdot a \cdot \rho$ the LL/Riemannian metric defined by (2) can be transformed into the gnomonic metric:

$$dl^3 = \frac{4}{\left(1 + \rho^2\right)^2}\left[d\rho^2 + \rho^2\left(\sin^2(\theta)d\varphi^2 + d\theta^2\right)\right] \text{ for } a = 1. \qquad (3)$$

3. Gnomonic holography of Two-Dimensional Surface

We will proceed with a very short illustration of what is well known as crystallo-graphic holography. Let the $\mathcal{S}^2$ manifold geometry correspond to

$$x^2 + y^2 + z^2 = 1$$

of curvature radius 1. The North Pole corresponds to the point

$$N_p = (0, 0, +1),$$

and the South Pole is denoted by

$$S_p = (0, 0, -1).$$

Conceive Euclidian plain $\mathcal{E}^2$ intersecting the origin

$$O = (0, 0, 0)$$

perpendicular to the z-axis. We can project a line from N through

$$(x, y, z) \in \mathcal{S}^2,$$

which will intersect the plain at a distance ρ from the origin O. Using $\mathcal{S}^2$ geometry it can be verified that

$$d^2 + z^2 = 1$$

what yields

$$d^2 = (1 - z)(1 + z).$$

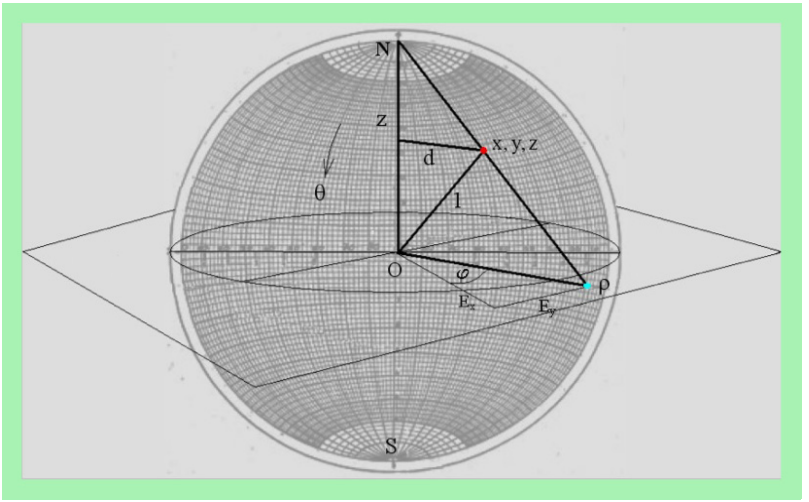

Figure 2. Surface $\mathcal{S}^2$ of the manifold $\mathcal{R}^3$ gnomonic holography at Euclidian Plane $\mathcal{E}^2$.

Now convert

$$\frac{d}{\rho} = \frac{1-z}{1}$$

into

$$d^2 = \rho^2 (1-z)^2 .$$

For latter d^2's these d^2 yield

$$z = \frac{-1+\rho^2}{1+\rho^2},$$

$$d = \frac{2\cdot\rho}{1+\rho^2}$$

what match up a 3-fold gnomonic holography, given by mapping

$$\left(\frac{2\cdot\rho}{1+\rho^2} \times \cos(\varphi); \frac{2\cdot\rho}{1+\rho^2} \times \sin(\varphi); \frac{-1+\rho^2}{1+\rho^2} \right)$$

of two variable functions as a diffeomorphism

$$S^2 \to \mathscr{E}^2$$

into Euclidian coordinates

$$(\mathscr{E}_x, \mathscr{E}_y)$$

on the plain

$$\mathscr{E}^2 : (\mathscr{E}_x, \mathscr{E}_y) = (\rho\cos(\varphi), \rho\sin(\varphi),$$

$0 \le \varphi \le 2\cdot\pi$, $0 \le \rho < \infty$.

Let us finally find the metric of our gnomonic holography drawn by Figure 2. The partial derivatives of the holography/diffeomorphism represent the Jacobin matrix J. The transpose of the matrix J is thus given by three functions of two variables:

$$J^T = \begin{Vmatrix} 2\cdot\frac{1-\rho^2}{(1+\rho^2)^2}\cdot\cos(\varphi); & 2\cdot\frac{1-\rho^2}{(1+\rho^2)^2}\cdot\sin(\varphi); & \frac{4\cdot\rho}{(1+\rho^2)^2} \\ -\frac{2\cdot\rho}{1+\rho^2}\cdot\sin(\varphi); & \frac{2\cdot\rho}{1+\rho^2}\cdot\cos(\varphi); & 0 \end{Vmatrix}.$$

Consequently, provided by Скляренко (2008), the metric tensor

$$G_{i,j} = J^T \times J, \text{ yields}$$

$$g_{i,j}d\rho^i d\varphi^j = \frac{4}{\left(1+\rho^2\right)^2}\begin{pmatrix} d\rho & 0 \\ 0 & \rho^2 d\varphi \end{pmatrix}.$$

Herby, in our $\mathcal{S}^2$ gnomonic topology $\mathcal{E}^2$ the rod element

$$dl^2 = \frac{4}{\left(1+\rho^2\right)^2}\left(d\rho^2 + \rho^2 d\varphi^2\right)$$

is represented on Figure 2. We will refer later to substitution

$$r = \frac{2\cdot\rho}{1+\rho^2}$$

representing the "*inverse*" part of the diffeomorphism of

$$\mathcal{S}^2 \to \mathcal{E}^2$$

or

$$\mathcal{S}^3 \to \mathcal{E}^3$$

gnomonic holography s, where dl^2 denotes the metric in the Euclidian plain $\mathcal{E}^2$. This means that it will be possible to refer to manifolds

$$\mathcal{S}^3(r) \equiv \mathcal{S}^3\left(\frac{2\cdot\rho}{1+\rho^2}\right),$$

which are now given as a function of ρ radius coordinate, and not of the radius r but as a holography radius ρ onto the Euclidean manifold $\mathcal{E}^3$, Figure 2.

4. Gnomonic holography of Three-Dimensional Surface

Unfortunately only a few people can conceive a four-dimensional hyper-manifold $\mathcal{R}^4$. However, the aforementioned process can be applied to a $\mathcal{S}^3$-dimensional surface of the $\mathcal{R}^4$ dimensional hyper-manifold. Around the North Pole

$$N_p = (0,0,0,+1)$$

as a reference system center, try to envision drawing an imaginary $\mathcal{S}^3(r)$ manifold given by polar coordinates of radius r, $0 \le r \le 1$. Our $\mathcal{S}^3(r)$ manifold is of a fixed curvature of radius 1. Proceed in similar way already described above for an ordinary manifold $\mathcal{R}^3$ encircling point N until the whole $\mathcal{S}^3$ surface of the $\mathcal{R}^4$ hyper-manifold is inflated.

Given at cosmological distances, the $\mathcal{S}^3$ surface of four-dimensional hyper-manifold $\Re^4$, the space $\mathcal{S}^3$ purported to be homogeneously inflated with energy and matter and is completely isotropic. The generic metric derivation, that meets these conditions, will be considered below only in case of closed model with positive curvature ≈ 1.

$$x^2 + y^2 + z^2 + r^2 = 1$$

These equations represent so-called closed space manifolds $\mathcal{S}^3(r)$ of curvature one on the surface enclosing four-dimensional hyper-hyper-manifold

$$\mathcal{R}^4 \qquad x^2 + y^2 + z^2 \le r^2 \le 1$$

The spherical coordinates x, y, z are related to the $\mathcal{E}^3$ coordinates by $\varphi = \tan^{-1}\left(\frac{y}{x}\right)$, $\theta = \cos^{-1}\left(\frac{z}{r}\right)$, with $r = \sqrt{x^2 + y^2 + z^2}$.

$x = r \cdot \cos(\varphi) \cdot \sin(\theta)$,
$y = r \cdot \sin(\varphi) \cdot \sin(\theta)$,
$z = r \cdot \cos(\theta)$, where
$0 \le r < 1$, $0 \le \varphi \le 2 \cdot \pi$,
and $0 \le \theta \le \pi$,

Given that a gnomonic diffeomorphism

$$\mathcal{S}^3 \to \mathcal{E}^3$$

maps S^3 into a quadruple of three-variable functions

$$\left(\mathcal{E}_x = \rho\cos(\varphi)\sin(\theta),\ \mathcal{E}_y = \rho\sin(\varphi)\sin(\theta),\ \mathcal{E}_z = \rho\cos(\theta)\right)$$

defined in spherical coordinates, where

$$0 \le \rho < \infty,\ 0 \le \varphi \le 2 \cdot \pi,$$

and $0 \le \theta \le \pi$, the gnomonic holography of S^3 from the North Pole

$$N_p = (0,0,0,+1))$$

identifies $\mathcal{R}^4$ with the hyperplane through the origin

$$O = (0, 0, 0, 0))$$

perpendicular to the line connecting N_p with South Pole

$$S_p = (0,0,0,-1):$$

$$\left(\frac{2\cdot\rho}{1+\rho^2}\times\cos(\varphi)\cdot\sin(\theta);\frac{2\cdot\rho}{1+\rho^2}\times\sin(\varphi)\cdot\sin(\theta);\frac{2\cdot\rho}{1+\rho^2}\times\cos(\theta);\frac{-1+\rho^2}{1+\rho^2}\right).$$

The partial derivatives of the holography/diffeomorphism represent the Jacobin matrix J, whereby its transpose J^T is given as follows:

$$J^T = \begin{Vmatrix} 2\frac{1-\rho^2}{\left(1+\rho^2\right)^2}\cdot\cos(\varphi)\sin(\theta) & 2\frac{1-\rho^2}{\left(1+\rho^2\right)^2}\cdot\sin(\varphi)\sin(\theta & 2\frac{1-\rho^2}{\left(1+\rho^2\right)^2}\cdot\cos(\theta & \frac{4\cdot\rho}{\left(1+\rho^2\right)^2} \\ -\frac{2\cdot\rho}{1+\rho^2}\cdot\sin(\varphi)\sin(\theta) & \frac{2\cdot\rho}{1+\rho^2}\cdot\cos(\varphi)\sin(\theta) & 0 & 0 \\ \frac{2\cdot\rho}{1+\rho^2}\cdot\cos(\varphi)\cos(\theta) & \frac{2\cdot\rho}{1+\rho^2}\cdot\sin(\varphi)\cos(\theta) & -\frac{2\cdot\rho}{1+\rho^2}\cdot\sin(\theta) & 0 \end{Vmatrix}$$

Consequently, Gram Matrix metric tensor $G_{i,j} = J^T \times J$ yields

$$g_{i,j,k}d\rho^i d\varphi^j d\theta^k = \frac{4}{\left(1+\rho^2\right)^2}\times\begin{Vmatrix} d\rho & 0 & 0 \\ 0 & \rho^2\sin^2(\theta)d\varphi & 0 \\ 0 & 0 & \rho^2 d\theta \end{Vmatrix},$$ which leads to rod element given by:

$$dl^3 = \frac{4}{\left(1+\rho^2\right)^2}\left[d\rho^2 + \rho^2\left(\sin^2(\theta)d\varphi^2 + d\theta^2\right)\right]. \qquad (4)$$

4.1. Geometric Encoding in Gnomonic Holography

Before approaching this issue, it is necessary to start calculating the volume of 3-dimensional regions in our 3-dimensional Euclidean plane $\mathscr{E}^3$. The following mathematical sequence is reduced to the following chain of formulas.

We know that in flat $\mathscr{E}^3$ topology, the volume rod dl^3 is equal to $dx \cdot dy \cdot dz$, whereas the rod length is given by

$$dl^2 = dx^2 + dy^2 + dz^2 .$$

Applying the same rule to the previous flat expression for dl^2, we obtain volume rod

$$dV = dl^3 \text{ as } dV = \sqrt{\det g} \cdot d\rho d\varphi d\theta :$$

$$g_{i,j,k} d\rho^i d\varphi^j d\theta^k = 8 \cdot \frac{\rho^2 d\rho \cdot \sin(\theta) d\theta \cdot d\varphi}{\left(1+\rho^2\right)^3}$$

within a coordinate triple: $0 \le \rho < \infty$, $0 \le \theta \le \pi$ and $0 \le \varphi \le 2\pi$. Hereby the expression in the form of integral represents the space volume $V(S^3_\rho)$ of a hyper-manifold $S^3(\rho)$ with a radius ρ.

$$8 \int_0^{2\pi} \int_0^{\pi} \int_0^{\rho} \frac{\xi^2 d\xi \cdot \sin(\theta) d\theta \cdot d\varphi}{\left(1+\xi^2\right)^3}$$

The *radius* $r = \frac{2 \cdot \rho}{1+\rho^2}$ can be interpreted as a new dimension, implying that the space volume is proportional to Euclidian space $\mathscr{E}^3$ at nearby distances. Taking the integral into account, we derive the expression of the volume:

$$V(S^3_\rho) = 4\pi \cdot \frac{-\rho + \tan^{-1}(\rho) + \tan^{-1}(\rho) \cdot \rho^4 + \rho^3 + 2 \cdot \tan^{-1}(\rho) \cdot \rho^2}{\left(1+\rho^2\right)^2} .$$

After accounting for the sub-expression $\tan^{-1}(\rho)$, we obtain

$$V(S^3_\rho) = 4\pi \cdot \frac{\left(1+\rho^4+2 \cdot \rho^2\right)}{\left(1+\rho^2\right)^2} \cdot \tan^{-1}(\rho) + 4\pi \cdot \frac{-\rho+\rho^3}{\left(1+\rho^2\right)^2} .$$

Finally, we arrive at $V(\mathcal{S}_\rho^3) = 4\pi \cdot \left(\tan^{-1}(\rho) + \rho \cdot \frac{-1+\rho^2}{\left(1+\rho^2\right)^2} \right)$.

In order to incorporate the Planck Mission 2018 satellite data into gnomonic holography, it is necessary to normalize (i.e., determine the proportion of) the volume $V(\mathcal{S}_\rho^3)$ with respect to the total volume $V(\mathcal{S}_\infty^3)$. Indeed, it is straightforward to verify that the volume of the entire space is given by

$$\lim_{\rho\to\infty} V(\mathcal{S}_\rho^3) = V(\mathcal{S}_\infty^3) = 2\cdot\pi^2,$$

Now it remains for us to calculate which part in percentage is the volume $V(\mathcal{S}_\rho^3)$ in relation to $2\cdot\pi^2$. To encompass the gnomonic holography in order to confirm to the matter composition put forward by the Planck Mission 2018 satellite data it is necessary to establish the normalized share% of the volume $V(\mathcal{S}_\rho^3)$ with respect to the entire volume $V(\mathcal{S}_\infty^3) = 2\cdot\pi^2$.

4.1.1. Synchronization of Internal Parameters by Means of a Dynamic System

A central role in the present framework is played by the dynamic system

$$F(\rho, \kappa, \lambda, \Delta),$$

whose nonlinear iterative structure governs the synchronization between the internal geometric parameters of the model and the observed cosmological composition of the Universe. The system is not introduced merely as a numerical fitting algorithm, but rather as a self-consistent dynamical mechanism through which physically admissible configurations are selected. In particular, the iterative root-finding mapping associated with $F(\rho, \kappa, \lambda, \Delta)$ must in the form (5) converge toward stable fixed points that reproduce the observational values determined by the Planck mission, namely the present-day density fractions Ω_c, Ω_Λ, Ω_b.

Within this framework, the cosmological energy composition is not imposed externally as an independent assumption. Instead, it emerges naturally as a consequence of the internal dynamics of the geometric-holographic structure. The convergence properties of the dynamic system therefore act as a physical selec-

tion principle: among all mathematically admissible parameter configurations (κ,λ,Δ), only those trajectories whose iterative evolution stabilizes at observationally consistent fixed points are retained. The observed Planck ratios, in this sense, become synchronization conditions dynamically enforced by the system itself.

The iterative mapping performs a dual function. Mathematically, it determines the coupled internal parameters κ, λ, and Δ through nonlinear interaction. Physically, it dynamically stabilizes the model around empirically viable states. The resulting fixed points, partition the radial domain into regions associated with dark matter, dark energy, and baryonic matter, thereby establishing a direct correspondence between the dynamical geometry of the model and the observed large-scale energy structure of the Universe.

We define the function

$$\Omega(\rho)=\frac{2}{\pi}\cdot\left(\tan^{-1}(\rho)+\rho\cdot\frac{-1+\rho^2}{\left(1+\rho^2\right)^2}\right),\ \text{around infinity}\ \Omega(\infty)=1,$$

where

$$2\cdot\pi^2\cdot\Omega(\rho)$$

represents the volume of a gnomonic three-sphere associated with the radius (rod) ρ.

The model assumes that matter originated through a phase transition of a primordial energy field, is described in normalized form by

$$\Gamma(\rho,\kappa,\lambda,\Delta)=-2\cdot\pi^2\cdot\kappa\cdot\Omega(\rho)+\Delta\cdot\rho^{\lambda}=0. \qquad (5)$$

Below, we introduce additional parameters: the energy-absorption κ-flow coefficient and the internal parameters Δ and λ, determined from the energy composition of the ΛCDM model through an interactive mapping procedure. We recall from **1.5** the standard 2018 Planck's results for the cosmological energy composition:

These parameter values, $\Omega_c\approx0.2640$, $\Omega_\Lambda\approx0.6847$ and $\Omega_b\approx0.0493$, provide the empirical baseline against which the predictive capability of the gnomonic holographic model is evaluated. We also will use $\Omega_d=\Omega_c+\Omega_b$: $\Omega_d\approx0.9487$—the dark sector (not standard, but acceptable shorthand).

The equations

$$\Omega(\rho)-\Omega_c=0 \text{ and } \Omega(\rho)-\Omega_b=0$$

must be solved with respect to ρ, starting from suitable initial guesses. This implicitly requires the use of an iterative procedure such as Newton's method or another numerical solver. The pair (ρ_c,ρ_b) partitions the radial domain $0\le\rho<\infty$ into three regions:

$$\Omega_c\approx 0\le\rho<\rho_c,\ \Omega_\Lambda\approx\rho_c\le\rho<\rho_b, \text{ and } \Omega_b\approx\rho_b\le\rho<\infty$$

corresponding respectively to the dark matter, dark energy, and baryonic matter sectors.

These sectors then generate a triple of nonlinear equations described by the trajectories of interest, $x\approx\kappa_i$, $y\approx\lambda_i$, and $z\approx\Delta_i$, as well as a triple of radii, ρ_c, ρ_b and $\rho_\Lambda=0$, emerged through density fractions Ω_c, Ω_b, where the latter $\rho_\Lambda=0$ denotes the singular solution of the Γ-equation:

$$\begin{cases}\Gamma(\rho_c,x,y,z)=0 & \text{given initial}\\ \Gamma(\rho_b,x,y,z)=0 & \text{guess to}\\ \Gamma(\rho_\Lambda,x,y,z)=0 & \text{be solved for}\end{cases}\quad (x\approx\kappa_{i+1},y\approx\lambda_{i+1},z\approx\Delta_{i+1}). \quad (6)$$

The resulting trajectory

$$i\to\infty\quad,(\kappa_i,\lambda_i,\Delta_i),$$

converge to the fixed point $\to(\kappa,\lambda,\Delta)$:

$$F\begin{pmatrix}\rho_c=0.670227254\\ \rho_b=3.061982489\end{pmatrix},\kappa=0.125046485,\begin{pmatrix}\lambda=0.850383059\\ \Delta=0.913196709\end{pmatrix},$$

which dynamically enforces the observed cosmological proportions. Only those trajectories of the dynamical system $F(\rho,\kappa,\lambda,\Delta)$ whose iterations converge to fixed points reproducing the Planck observational values $(\Omega_c,\Omega_\Lambda,\Omega_b)$ are retained. In this formulation, the observed cosmic composition emerges as a consistency condition imposed by the underlying geometric-holographic structure, rather than as an independent external input.

The fixed points of the mapping

$$(\rho,\kappa,\lambda,\Delta)\to F(\rho,\kappa,\lambda,\Delta)$$

arise naturally within the framework of gnomonic holography, in which higher-dimensional geometric configurations manifest as observable physical phenomena. Within this interpretation, cosmic expansion is understood not merely as a kinematic effect, but as a consequence of an underlying geometric constraint structure.

Accordingly, the "inside" region $(\rho < \rho_c)$ of KB is associated with the dark matter sector, whereas the "outside" region $(\rho > \rho_b)$ corresponds to baryonic matter. The intermediate domain encodes dark energy. The associated angular ranges are $0 \le \theta \le \pi$, $0 \le \varphi \le 2\pi$. We further argue that, along the absorption κ-flow, the parameter value $\kappa' \approx 0.125046486$ satisfies

$$(\kappa_\infty > ... > \kappa' \approx 0.125046486 > ... > \kappa^\bullet \approx 0.877272830,$$

which corresponds to the present Planck mass–energy budget. Although this value was not independently derived and represents a non-comprehensive value of the parameter, the parameter nevertheless has predictive power.

In fact, a decrease in $\infty \to \kappa$ predicts the *"death"* of the universe while $\rho_c = \rho_b = \rho_\bullet \approx 1.311806779$, $\kappa \to \kappa^\bullet$, $\Omega_\Lambda \to \varnothing$ and $\kappa^\bullet \approx 0.087273587$. Approaching the BB along $k \to \infty$, the ratio

$$\frac{\Omega_c}{\Omega_b}$$

of dark matter per unit of visible matter rises, in contrast, to $\approx 1.4 \cdot 10^9$ at $\kappa \approx 10^3$, showing that dark matter overwhelmingly dominated baryonic matter near the Big Bang.

It remains to examine once more the connection between the metric space—interpreted here as a gnomonic holography—and its original pre-image defined by the Landau–Lifshitz metric (1). As previously noted, metric (1) appears to represent two ″bubbles″ extending along the coordinate **r**: one obtained by increasing **r** from **0** to **1**, and the other by decreasing **r** from **1** to **0**. This behavior may be heuristically understood as a transition from the ″inside″ to the ″outside″ of the Klein bottle along the coordinate **r**. This interpretation becomes more transparent under the substitution

$$r = \frac{2 \cdot \rho}{1 + \rho^2}, \tag{7}$$

where $[0 \le \rho < \infty)$ parameterizes the gnomonic interval. Within the gnomonic holographic picture, these two bubbles are clearly separated—analogous to the interior and exterior of the Klein bottle—by the transition boundary at r =1. In contrast, within metric (1), the two bubbles are superimposed, each possessing a volume π^2.

For heuristic purposes, the non-orientable topology of the Klein bottle may be described in terms of ″inside″ and ″outside″ regions represented as two overlapping domains within the gnomonic interval $[0 \le \rho < \infty)$.

These domains may be visualized as interpenetrating regions distributed along the boundary $\rho = 1$, overlapping at all points $(\mathscr{E}_x, \mathscr{E}_y, \mathscr{E}_z)$ equidistant from the common center. Each region is associated with an effective volume π^2, emphasizing their topological equivalence and the absence of a globally well-defined interior–exterior distinction. The reader may verify this correspondence by substituting (7) into equation (1), which yields metric (3) and, consequently, metric (4), in agreement with the derivation given above.

It remains for us once again to pay attention to the connection between the metric space, which is a gnomonic holography, and the original (pre-image) defined by the Landau-Lifshitz metric (1). As already noticed, in metric (1), there seem to be two bubbles extending along the coordinate r when moving along r from zero to 1, and in the opposite direction from 1 to zero. This movement along the coordinate r will be clear from the substitution (7), when moving along the coordinate ρ within the gnomonic interval $[0 \le \rho < \infty)$. In gnomonic holography, as said, these two bubbles are clearly separated by the transition boundary when $r = 1$. In metric (1), however, these two bubbles are hyper-imposed on each other and each of which has a volume of π^2.

In order to be convinced of the above, we need to calculate the volume of the 3D manifold $V(S_r^3)$, which extends in metric (1) normalized within the interval $[0, r)$.

Indeed

$$\overline{\Omega}(r) = \int_0^{2\pi} \int_0^{\pi} \int_0^{r} \frac{\xi^2 d\xi \cdot \sin(\theta) d\theta d\varphi}{\sqrt{1-\xi^2}} = \pi^{-1}\left(\sin^{-1}(r) - r \cdot \sqrt{1-r^2} \right),$$

for $r \in (0...1]$, $\overline{\Omega}(1) = ½$.

Proposition. Under the coordinate transformation

$$r = \frac{2 \cdot \rho}{1 + \rho^2}, \ [0 \le \rho < \infty),$$

the Landau–Lifshitz metric (1) is mapped into the gnomonic metric (3), thereby realizing a gnomonic projection equivalence with Riemannian metric in the form of gnomonic holography of four-dimensional hyper-manifold $\mathcal{R}^4$ onto the Euclidean space $\mathcal{E}^3$. Indeed, applying the substitution

$$r = \frac{2 \cdot \rho}{1 + \rho^2},$$

we obtain just testing that:

- $\Omega(\rho_c) = \overline{\Omega}(r_c) = 26.40\%$
- $100\% - \Omega(\rho_b) = \overline{\Omega}(r_c) = 4.93\%$ and
- $\Omega(\rho_b) - \Omega(\rho_c) = 100\% - \left(\overline{\Omega}(r_c) + \overline{\Omega}(r_b)\right)$

These equals correspond to a proposed relationship between volumes in the Riemannian metric and holographic descriptions, expressed in gnomonic coordinates, and are claimed to match the mass–energy budget observed by the Planck mission.

These values underscore the significant dependence of observational interpretation on the underlying our theoretical framework. The stereographic Landau-Lifshitz (LL) metric offers an alternative geometric perspective for understanding cosmic evolution,

$$\text{for } \rho_c = 0.670227254, \text{ and for } \rho_b = 3.061982489.$$

These ρ's values originate from the postulate of so called zero-point-field (ZPF) phase transition into baryonic and dark matter (Mullat, 2022, illustration on Figure 2):

$$\overline{\Omega}\left(r_c = \frac{2 \cdot \rho_c}{1 + \rho_c^2}\right) = 0.2640, \text{ and } \overline{\Omega}\left(r_b = \frac{2 \cdot \rho_b}{1 + \rho_b^2}\right) = 0.0493.$$

4.2. Gnomonic Holography and a Hubble-like constant

Consider a normalized volume $\Omega(\rho)$, where ρ represents the length of a rod extending from a point on the 3D super-sphere embedded in a 4D manifold. This rod is associated with a differentially small 3D area element $d\Omega(\rho)$ at its apex. Suppose the rod increases infinitesimally in length by $\rho \cdot d\rho$.

Because of averaging and evolution do not commute, the Hubble's H_0 expansion rate inferred from observations is an effective, scale-dependent quantity determined by how local inhomogeneities are averaged into a global description (Buchert, 2007). Therefore, by our assumption, this increment is proportional to the corresponding change in the supersphere differential, such that

$$\rho \cdot d\rho = H_0 \cdot d\Omega(\rho),$$

where H_0 is a Hubble-like constant of proportionality. It follows that

$$\rho = H_0 \cdot \dot{\Omega}(\rho).$$

where $\dot{\Omega}(\rho)$ denotes the rate of change of the volume with respect to ρ. Using the gnomonic holographic formulation, $\dot{\Omega}(\rho)$ can be expressed as

$$\dot{\Omega}(\rho) = \frac{2}{\pi}\frac{d}{d\rho}\left(\tan^{-1}(\rho) + \rho \cdot \frac{-1+\rho^2}{\left(1+\rho^2\right)^2}\right), \text{ or as } \dot{\Omega}(\rho) = \frac{16}{\pi} \cdot \frac{\rho^2}{\left(1+\rho^2\right)^3}, \quad (8)$$

(or equivalently via an alternative trigonometric form).

Think of ΛCMD model universal "ruler expansion function":

If $\dot{a} > 0$ increases → the universe expands;
If $\dot{a} < 0$ decreases → the universe contracts;
If $\dot{a} = 0$ stays constant → static universe.

Looking at expansion rate with ΛCMD the Hubble parameter

$$H(t) = \frac{\dot{a}(t)}{a(t)}.$$

Using $\dot{\Omega}(\rho)$ coming from $\Omega(\rho)$ coordinate ρ by analogy but though the gnomonic relation for the Hubble parameter, the parameter becomes

$$H_0(\rho) = \frac{\rho}{\dot{\Omega}(\rho)},$$

which represents, however, a reciprocal of $H(t)$. Given the expression (8) the

$$H_0(\rho) = \frac{\pi}{16 \cdot \rho} \cdot \left(1+\rho^2\right)^3.$$

4.2.1. The Hubble Tension

The so-called Hubble tension refers to the persistent discrepancy between different measurements of the present-day expansion rate of the Universe, H_0. Observations of the early Universe, particularly those derived from the cosmic microwave background measured by the Planck Collaboration, consistently predict a lower value of H_0, while late-Universe measurements based on visible astrophysical objects yield a higher value.

Considering the present cosmological energy balance, the combined dark-sector Ω_d contribution may be written as

$$\Omega_d = \Omega_c + \Omega_\Lambda \approx 94.87\%.$$

Meanwhile the complementary fraction obtained by excluding only baryonic matter

$$\Omega_b \approx 4.93\% \text{ is } 100\% - 4.93\% = 95.07\%.$$

This leaves a small residual difference of approximately 0.2%, potentially indicating a slight imbalance when late-time observational and CMB-derived datasets are compared.

Within the proposed framework, this difference corresponds to a separation $\rho_b - \rho_d$ in gnomonic radii of roughly 0.046 gnomonic units, associated with characteristic visible or baryonic matter Ω_b and dark sector Ω_d fractions′ imbalance:

$$\rho_b \approx 3.062 \text{ vs. } \rho_d \approx 3.016 \text{ respectably.}$$

For the function $H_0(\rho)$ we obtain

$$H_0(\rho_b) \approx 71.63, \text{ and } H_0(\rho_d) \approx 67.04.$$

The difference,

$$71.63 - 67.04 = 4.59,$$

which is noticeably close to the mystery, although it still remains speculative.

Based on what we have shown, $\rho(\Omega)$ acts as a coordinate, while $H_0(\rho)$ serve as a scale factor to change by an amount of order if the current expansion rate reciprocal

$$t(\rho) = \frac{1}{H_0(\rho)}$$

defines an emergent timescale associated with the geometry.

For the values $\rho_c \approx 0.670227$ and $\rho_b \approx 3.061982$, this construction yields

$$\frac{t(\rho_c)}{t(\rho_b)} \approx 80.3 .$$

Because the radii ρ are derived independently from the underlying Ω-based geometry, this result suggests, in holographic terms, that the visible and dark sectors may be associated with different characteristic timescales.

If the cosmic clock is identified with the inverse Hubble scale $t(\rho)$, the corresponding clock function takes the form

$$t(\rho) = \frac{16 \cdot \rho}{\pi \cdot \left(1 + \rho^2\right)^3} .$$

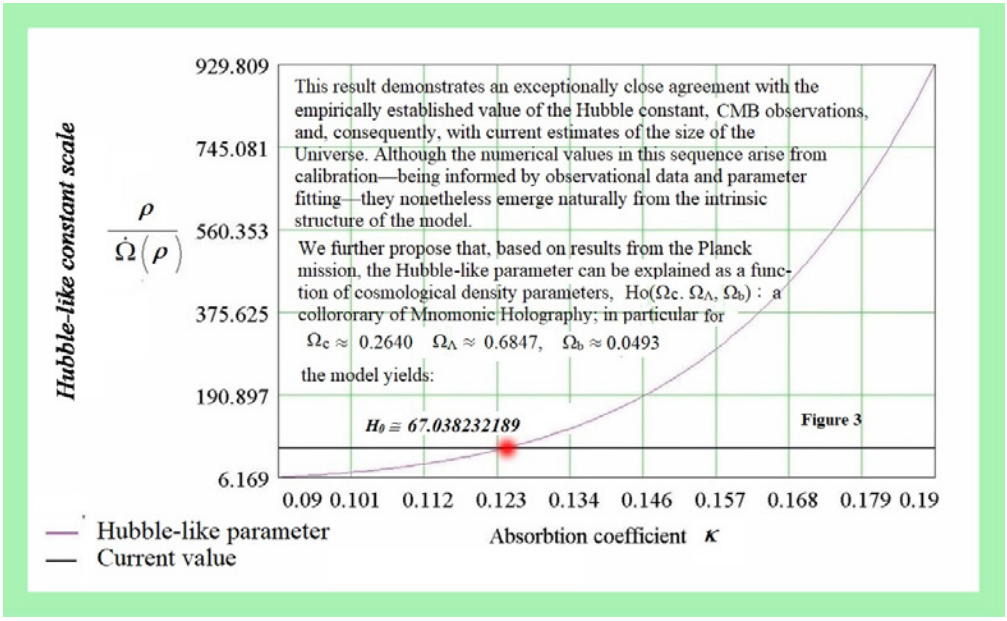

Within this framework, the factor of approximately 80.3 emerges naturally from the geometric construction rather than being imposed externally. The clock function exhibits two distinct regimes. Near the origin, the timescale varies approximately linearly with ρ. At larger radii, however, it decreases rapidly, scaling asymptotically as ρ^{-5}. This behaviour suggests that ρ may encode more than spatial information alone; it may also regulate the characteristic rate at which a sector evolves.

An important question remains. Are the values $\rho_c \approx 0.670227$ and $\rho_b \approx 3.061982$ obtained independently from dark-matter abundance and geometric considerations, or do they arise from assumptions that implicitly enforce a particular visible-to-dark matter ratio? The answer is significant because it determines whether the factor of approximately 80.3 should be regarded as a genuine prediction of the model or as a consequence of the way the characteristic radii are defined.

Under this interpretation, two possible readings emerge.

1. Expansion-timescale interpretation in the more conservative interpretation $t(\rho)$ represents a characteristic evolutionary timescale rather than the flow of proper time itself.
   - The dark sector is associated with an evolution timescale approximately 80.3 times longer than that of the visible sector.
   - As a consequence, the formation and evolution of large-scale structures would proceed more slowly when measured against the corresponding cosmological timescale.
2. Physical-clock interpretation gives a stronger interpretation is that $t(\rho)$ represents an actual sector-dependent clock.
   - Proper time in the dark sector would then be rescaled by a factor of approximately 80.3 relative to the visible sector.
   - According to this hypothesis, a process lasting one tick in the visible sector will correspond to approximately 0.0125 ticks in the dark sector, and vice versa — one tick in the dark sector will correspond to approximately 80.3 ticks in the visible sector.

The distinction between these interpretations is fundamental. The first concerns differences in dynamical evolution rates and follows directly from the emergent timescale construction. The second attributes physical significance to those timescales as sector-dependent rates of temporal flow. Whether the model supports this stronger interpretation remains an open question and would require additional theoretical and observational justification.

Conclusion. We argue that this value of the Hubble-like constant is not merely a fitted parameter, but an intrinsic consequence of gnomonic holography combined with the hypothesis that matter emerged from a primordial energy field suggesting that the Hubble-like constant may be understood as a geometric consequence of the model rather than an independently imposed observational constant.

Although this interpretation remains speculative, it suggests that the Hubble tension may originate from a small discrepancy of approximately 0.2% between the dynamics of observable (baryonic) matter and the gravitational effects associated with the dark sector. Within the proposed framework, this difference may reflect a subtle imbalance that is not fully captured by the conventional separation between baryonic matter and dark matter–dark energy components. In this sense, the framework may offer a possible avenue toward explaining why different observational methods infer slightly different values of the Hubble constant.

4.3. Predictive Power of the Proposed Cosmological Framework Revisiting the section 1.5

It is now well-established that the Universe is undergoing accelerated expansion—a phenomenon first discovered through supernova measurements by Saul Perlmutter, Brian P. Schmidt, and Adam G. Riess, who were awarded the 2011 Nobel Prize in Physics for this work. We employ the Γ-equation (5) as the predictive core in those analogies lines, treating its mapping abilities within the mnemonic holography black box, where empirical reality provides the input. Rather than calibrating the equation to fit observations, the requirement is that the model, when evaluated under physical conditions, encompasses the Planck results as an intrinsic consistency condition. Specifically, we impose $\Gamma(\rho, \kappa, \lambda, \Delta) = 0$ and adopt the parameter values:

$$\kappa' = 0.125046486,\ \lambda = 0.843370586, \text{ and } \Delta = 0.913196709.$$

Within this interpretation, κ' is not a fitted parameter but emerges as the present-day absorption coefficient, defining the reference (zero) point of the κ-flow. In this framework, κ evolves over the history of the Universe, transitioning from higher to lower values through cosmic development. Deviations from the reference value $\kappa' = 0.125046486$ –whether toward larger or smaller values–encode information about the energy–matter budget at different stages of cosmic evolution. This last value can therefore be interpreted as the present-day absorption coefficient defining the zero point of the κ-flow.

The central parameter of the model is κ, interpreted as the rate of energy absorption from the zero-point field (ZPF). The value $\kappa' = 0.125046486$ serves as a critical point that partitions the κ-flow into two regimes (κ-flow future and κ-flow past):

- $\kappa < \kappa'$— which indicate evolution toward the terminal phase of the Universe.
- $\kappa > \kappa'$— which corresponds to evolution in the opposite direction, approaching the initial conditions associated with the Big Bang.

Thus, the Γ-framework functions not as a calibrated fit, but as an interpretive structure in which the observed Universe is processed through the model, and κ acts as the organizing parameter of cosmological time and state.

4.4. Interpreting Cosmic Expansion with Gnomonic Holography

To conclude, we summarize and interpret the calculated results, which are presented in Table 1 in the context of the preceding phenomenological sections and the mathematical framework employed. Our speculative interpretation of dynamic expansion—along with the increasing and decreasing acceleration—may seem ambitious, but it is conceptually straightforward and does not rely on advanced computational methods. This simplicity, as promised at the outset, is central to our proposed framework.

What follows is a truly intriguing and bold concept with deep philosophical and scientific implications. We hope it will be more accessible to a wider audience, especially those not well versed in advanced cosmology or philosophical theory. The text preserves the core ideas of the article while making it flow more smoothly, cutting down on technical jargon, and emphasizing the novelty of our thoughts.

Table 1. The Universe Kinematic and Cosmological Indicators

Category	Value $\Omega_i(\rho)$	Gnomonic Radius	Ω_i Value	Ho Resemble	*Kappa* Flow
Acceleration maximum (dark matter) and its non-	$\ddot{\Omega}_c(\rho)$	$\rho^a_{max} = 0.286547$	1.779117	0.868255	0.470216
extremal counterpart (visible matter)	$\ddot{\Omega}_b(\rho)$	15.939145	N/A	294396.46	
Acceleration minimum (dark matter) and its non-	$\ddot{\Omega}_c(\rho)$	$\rho^a_{min} = 1.103581$	−0.667009	1.941092	0.089531
extremal counterpart (visible matter)	$\ddot{\Omega}_b(\rho)$	1.1617909	N/A	5.745763	
Velocity maximum (dark matter) and its non-	$\dot{\Omega}_c(\rho)$	$\rho^v_{max} = 0.707635$	0.754512	0.937171	0.118923
extremal counterpart (visible matter)	$\dot{\Omega}_b(\rho)$	2.865216	N/A	53.527344	
Current state (dark matter velocity and acceleration rates)	$\dot{\Omega}_c(\rho_0)$ $\ddot{\Omega}_c(\rho_0)$	0.675546	0.752439 0.133496	0.898101	0.124591
Current state (visible matter velocity and acceleration rates)	$\dot{\Omega}_b(\rho_1)$ $\ddot{\Omega}_b(\rho_1)$	3.069028	0.042413 −0.047545	72.360027	

- The maximum of expansion rate velocity, and both the maximum positive acceleration and its minimum (negative) acceleration rates, corresponding to a phase of deceleration in the cosmic expansion. The model yields the values: velocity $\dot{\Omega}(\rho_b) = 0.04250418$, acceleration $\ddot{\Omega}(\rho_b) = -0.047545094$.
- These values indicate a reduction in the acceleration of cosmic expansion. Within this framework, the theoretical model offers a novel interpretation of the distinct expansion behaviors of baryonic matter and dark (hidden) matter,
- Specifically: Baryonic matter continues to expand, but its expansion rate is decelerating. Dark (hidden) matter, by contrast, expands with positive acceleration. This dichotomy is consistent with observational results reported by Saul Perlmutter and collaborators regarding cosmic expansion measurements. Moreover, reg. the visible universe.

*"Scientists have long held that the universe is expanding at an ever-increasing rate, driven by a mysterious but measurable force known as dark energy. Now, a new study might upend that idea, suggesting the universe's expansion is actually slowing down—and that dark energy is diminishing, rather than stable."…*Smithsonian magazine, accessed 27.02.2026:

https://www.smithsonianmag.com/smart-news/the-universes-expansion-may-be-slowing-down-not-speeding-up-new-research-suggests-180987660/

Given κ-flow acceleration, where κ is determined the dynamic operator as in (6):

$$\ddot{\Omega}(\rho) = \frac{2}{\pi}\frac{d^2}{d\rho^2}\left(\tan^{-1}(\rho) + \rho\cdot\frac{-1+\rho^2}{\left(1+\rho^2\right)^2}\right) \text{ or.}$$
$$\ddot{\Omega}(\rho) = -\frac{32}{\pi}\cdot\rho\cdot\frac{\left(-1+2\cdot\rho^2\right)}{\left(1+\rho^2\right)^4} \quad (9)$$

Maximum of

$\ddot{\Omega}_c(\rho^a_{max})$ at $\rho^a_{max} = 0.286546969$; the value 1.779116815 is reached when $\Gamma(\rho^a_{max}, \kappa, \lambda, \Delta) = 0$ with respect to κ, yielding κ=0.469443328.

Minimum of $\ddot{\Omega}_c(\rho^a_{min})$ at

$\rho^a_{min} = 1.103580914$, the value −0.667009510 is reached when

$\Gamma(\rho^a_{min}, \kappa, \lambda, \Delta) = 0$ with respect to κ, yielding κ=0.089504773;

Maximum of $\dot{\Omega}_c(\rho^v_{max})$

at $\rho^v_{max} = 0.707635257$, the value 0.754512323 is reached when

$\Gamma(\rho^v_{max}, \kappa, \lambda, \Delta) = 0$ with respect to κ, yielding κ=0.118923185.

The table compiles key indicators related to velocities, accelerations, and characteristic radii, alongside their corresponding values on the κ-flow. Each quantity is derived from the governing function Ω and its derivatives, evaluated at specific radii.

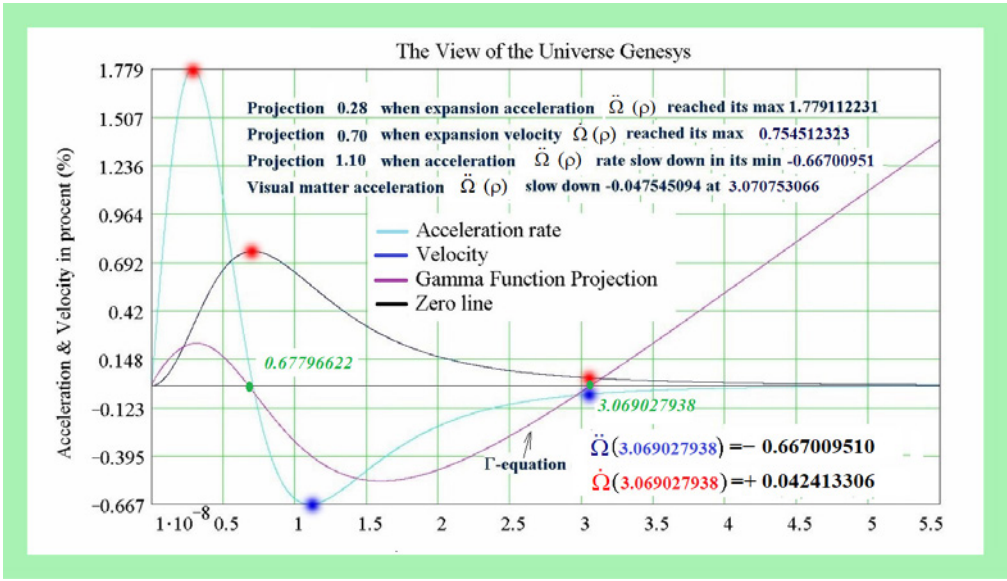

Figure 4 illustrates together with Table 1 the dynamics of the universe's volume $V(S^3_\rho)$ expansion's rate $\dot{\Omega}(\rho)$ (the velocity) on the normalized flow—expression (8)—together with expression (9), which describe and acceleration rate $\ddot{\Omega}(\rho)$ as functions of the gnomonic holography coordinate ρ.

The figure highlights several important points in the model dynamics. In particular it represents a situation in which the parameter κ acts as a player capable of predicting its value at which a point on the graph will be reached. To determine this value, the gnomonic coordinate ρ must be substituted into the Γ-equation (5) corresponding to the points where the extreme occur: the maximum of the velocity rate $\dot{\Omega}(\rho^v_{max})$; the maximum of the acceleration rate $\dot{\Omega}(\rho^a_{max})$, and the minimum of $\ddot{\Omega}(\rho^a_{min})$. The resulting equations are then solved for κ. The following Table 1 yields Figure 4 content.

A central feature of the model is that the Γ-equation yields two roots, denoted ρ_c and ρ_b, with $\rho_c \leq \rho_b$. The limiting case $\rho_c = \rho_b$ is not excluded and corresponds to a terminal state in which dark energy is fully depleted. Within this framework,

- ρ_c is interpreted as the radius associated with cold (dark) matter,
- ρ_b which corresponds to the radius of baryonic (visible) matter.

Accordingly, all numerical values in Table 1 appear in pairs, representing first the dark matter component and then the visible matter component. Each indicator is computed based on these radii.

Only quantities exhibiting a local extreme (maximum or minimum) within the considered radial interval are included in the table. This selection criterion is consistent with the behavior illustrated in Figure 4. Notably, functions associated with visible matter do not always exhibit local extreme within this interval of interests and are therefore omitted in such cases.

Figure 4 is a direct graphical representation of the quantitative results summarized in Table 1. Specifically, the figure visualizes the behavior of the universe's expansion dynamics—both the velocity and acceleration rates—derived from the same governing functions whose key extreme and corresponding parameter values are listed in Table 1. Each critical point shown in Figure 4 (such as maxima and minima of velocity and acceleration rates) corresponds exactly to entries in Table 1, where their numerical values, associated radii, and κ-flow parameters are reported.

In this sense, Table 1 provides the precise numerical backbone of Figure 4: the extrema identified analytically from the governing equations are plotted in the figure to illustrate their role in the overall dynamical evolution. Conversely, Figure 4 offers a visual interpretation of Table 1, showing how these discrete values fit into continuous curves of velocity and acceleration rates as functions of the gnomonic coordinate.

Moreover, the κ-values listed in Table 1 determine the exact locations of these extrema on the curves in Figure 4. By substituting the corresponding radii into the governing equations and solving for κ, one obtains the same parameter values that locate the highlighted points in the figure. This establishes a one-to-one correspondence between the tabulated indicators and the graphical features.

Overall, the results summarized in Table 1 appear to reflect a consistent dynamical picture of the universe's evolution. The model does not contradict current observational understanding and, in several respects, aligns with established descriptions of cosmological dynamics.

Thus, Table 1 and Figure 4 should be read together: the table identifies and quantifies the key dynamical events, while the figure situates them within the global evolution of the model.

We now turn to the κ-flow parameter. As established throughout the paper, the value

$$\kappa' = 0.125046486$$

represents the current state of the universe within the proposed κ-flow framework. Values of κ greater than this reference κ' correspond to earlier cosmological stages (closer to the Big Bang), while smaller values correspond to later stages, approaching the final state of matter in the universe. This parameterization enables a unified interpretation of all events represented in Table 1 along a temporal-like κ-flow, encompassing both past and future states of the system.

From these results, the following conclusions may be drawn. In case when if the absorption coefficient according to Planck is taken as current $\kappa' = 0.125046486$ the event corresponding to $\kappa = 0.469443328$ lies at a value greater than the Planck reference and may therefore be interpreted as belonging to an earlier cosmological epoch, closer to the Big Bang. In case when, the event associated with $\kappa = 0.089504773$ lies below the Planck reference value and may be interpreted as occurring in the future, toward the ultimate thermodynamic fate of the universe. In case when, the event corresponding to $\kappa = 0.118835137$, associated with the maximum relative expansion velocity of the universe, lies sufficiently close to the present Planck reference state of mass–energy budget to suggest that it will occur *relatively soon* on our cosmological κ-flow.

5. An Alternative Perspective on the Universe: Genesis, Expansion, and Infinite Evolution

Our stimulating idea endorses an alternative picture of the Big Bang. We propose that the expansion of the Universe is not simply about space stretching—but rather a grand phase transition, a shift that created both visible and dark matter. This transition emerged from a deeper, four-dimensional energy field we call the zero-point-field (ZPF)—a kind of fundamental background energy, invisible yet foundational. This creation process wasn't explosive. Instead, it unfolded through a sequence of evolving three-dimensional ″slices″ of space—mathematical shapes known as three dimensional (3D) manifolds

$$(\varnothing \approx S_0^3 \subset S_1^3 \subset, \ldots, \text{and so on till} \subset S_\bullet^3)$$

—each one larger than the last. These manifolds reflect, or are ″golographed″ from, the 4D ZPF and help us understand the growth of the Universe using the FLRW manifold metric's Riemannian slices—a standard geometry in cosmological models that describes the large-distance symmetrical structure of space and time. In this view, the so-called ″Big Bang″ wasn't a Bang at all. Our first postulate is that after their creation, the visible and dark matters were essentially at rest—no initial explosion, just emergence.

Our second postulate deals with the energy exchange between the Universe and the ZPF. While the Universe continues to expand, its ability to absorb energy from the ZPF gradually decreases. In simpler terms: the larger the Universe gets, the less it draws from this infinite source. We describe this behavior through a property we call the average absorption coefficient, denoted by κ, which declines as expansion progresses.

Philosophically, this idea echoes Spinoza's radical notion: that God is not the creator of the Universe, but rather that the Universe is God itself—everything that exists is a manifestation of this one infinite substance. While such thinking has historically clashed with mainstream religious views, we find a bridge in the ideas of the Danish philosopher Søren Kierkegaard, especially his concept of synthesis—the idea that apparent opposites can exist together in a deeper unity.

This leads us to our core equation, the Γ-equation (5), and expressed as: $\Gamma(\rho, \kappa, \lambda, \Delta) = 0$. Solving this equation allows us to describe a new kind of cosmic distance—one that exists beyond time, as we know it. It doesn't track the motion of objects through space, like in Newtonian or Einsteinian models. Instead, it maps the structure of the Universe itself—its division into components, their genesis, and their evolution.

Ultimately, this framework lets us envision both the beginning and the end—the creation and the eventual death—of the Universe, not as a timeline of events, but as a dynamic interplay of existence and energy rooted in a deeper, unseen dimension.

6. Concluding Remark

Crucially, the observed Planck mission cosmic recipe (baryonic matter: **4.93%**, dark matter: **26.40%**, and dark energy: **68.47%**) depends on how data is interpreted within a theoretical framework. The Landau-Lifshitz (LL) Stereo-Graphical metric space provides an alternative geometric structure for understanding the universe's evolution (Figure 5). Unlike the conventional Riemannian interpretation, which constrains observations to fit within its assumed framework, the LL/Riemannian approach offers a more adaptable perspective, making it better suited to accommodate recent JWST discoveries.

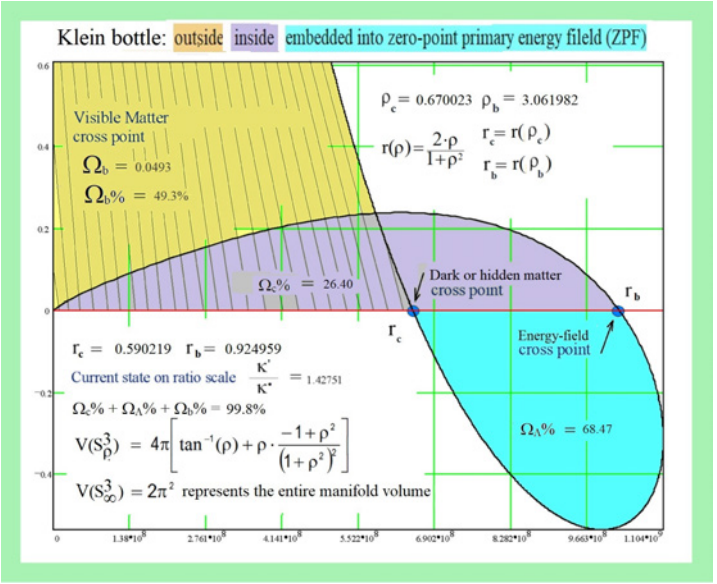

Figure 5. Planck Mission data $\mathcal{S}^3$ holography of hyper-manifold $\mathcal{R}^4$ at Plane $\mathcal{E}^3$.

In light of these challenges, alternative approaches—such as a gnomonic holography interpretation of the Riemannian manifold metric space, combined with the author's Monotonic Systems theory (Mullat, 1976–1977)—may provide a more comprehensive account of cosmic dynamics. We contend that viewing cosmological time as an extrapolated coordinate rather than a directly observable quantity constitutes a philosophically legitimate critique, one that aligns with longstanding concerns in both general relativity and quantum gravity.

The novelty of current approach lies primarily in a shift of perspective. Rather than focusing on what is traditionally expected of cosmological theories—namely, the prediction of the motion of material bodies in space—we concentrate on the structural origin of the Universe itself. However, some of the remarks enclosed with the manuscript reflect a common criticism, specifically the absence of a detailed treatment of matter dynamics and of an explicit κ-flow parameter governing such dynamics. In our view, these issues are not central to the objectives of the present article. Accordingly, the work does not address the dynamical evolution of individual cosmological objects, but instead focuses on the entity and geometric structure from which the Universe arises.

The article offers a description of the Universe's global structure and its large-flow evolution, including phenomena that may remain invisible beyond the limits of present observational horizons. Mathematics plays a central role in this analysis, serving as a bridge between two well-established frameworks: gnomonic visualization methods and the Riemannian Manifold metric. We argue for a structural identity between these two categories, drawing in part on observations by Landau and Lifshitz in The Classical Theory of Fields as they relate to cosmology.

This perspective would not, in our view, merit presentation—particularly given its mathematical content—unless it were grounded in empirical observation and supported by established theoretical considerations; relevant observational indications include, for example, the statistical comparison of angular diameter distances between quasar pairs reported in Mullat and Noble (2022, https://www.datalaundering.com/download/Fundamental-RG.pdf, "An Experiment Comparing Angular Diameter Distances Between Pairs of Quasars", ISBN-13 9789403674216, accessed 09.03.2026), although the detailed analysis lies beyond the scope of current presentation.

It is widely accepted in the literature, and frequently emphasized in lectures by leading cosmologists, that the observable Universe is not only expanding but doing so at an accelerating rate. This accelerated expansion emerges naturally from the mathematical framework developed in the manuscript. Within this framework, the Big Bang is not interpreted as an explosion, but rather as a rapid phase transition.

From this perspective, recent observations—such as the presence of apparently very old galaxies at high redshift revealed by the James Webb Space Telescope—are no longer paradoxical. In a phase-transition framework, successive transitions may occur that are not ordered as a conventional temporal sequence. Early stages of such a sequence may already correspond to states containing well-formed galaxies, contrary to expectations derived from standard cosmological narratives.

Acknowledgement

The mathematical derivation that originally motivated this work—now rendered obsolete—was first presented at the seminar of M.A. Aizerman, È.M. Braverman, and L.I. Rozonoèr in Moscow in 1973. The author is grateful for these early intellectual contexts in which the initial ideas were explored. Appreciation is also extended to Forrest Noble for the insightful ″Cosmological talks″ held during his visit to Copenhagen in March 2022, which contributed to the broader perspective underlying the present work.

Earlier versions of the derivation have appeared on various public-domain platforms (e.g., ResearchGate). However, the current article removes outdated elements and significantly advances the original formulation through the introduction of a new interpretation. As such, it should be regarded as an independent publication, with less than one third of the earlier material retained in revised form.

Literature cited

Aghanim, N. (2020) et al. Planck 2018 results. VI. Cosmological parameters (Planck Collaboration), *Astronomy & Astrophysics* **641**, A6, Preprint: arXiv:1807.06209.

Brans, C. & Dicke, R.H. (1961), ″Mach's Principle and a Relativistic Theory of Gravitation″, Physical Review.

Buchert, T. (2007) "Backreaction Issues in Relativistic Cosmology and the Dark Energy Debate," AIP Conf.Proc. 910 1, 361-380.

Danilatos, G.D. (2020) Novel quantitative push gravity/field theory poised for verification. North Bondi, Australia: ESEM Research Laboratory, https://zenodo.org/records/18112197, 25.01.2026.

Diaz, Pablo, Per, M.A. and Antonio Segui (2007) Fischler-Susskind holographic cosmology revisited, Departamento de Fisica Teorica, Universidad de Zaragoza. 50009-Zaragoza. Spain.

Edwards, Matthew R. (2002) Pushing Gravity: New Perspectives on Le Sage's Theory of Gravitation, editor, ISBN 9780968368978, https://www.amazon.co.uk/gp/search?index=books&linkCode=qs&keywords=9780968368978

Ellis, G.F.R. (2014) Relativistic cosmology: its nature, aims and problems. In: Ellis, G.F.R., Maartens, R. and MacCallum, M.A.H. (eds.) Relativistic Cosmology. Cambridge: Cambridge University Press, pp. 1–38.

Fischler W. and Susskind L. (1998) Holography and Cosmology, Theory Group, Department of Physics,University of Texas, and Austin,TX 78712, Department of Physics, Stanford University, Stanford, CA 94305-4060.

Fritz Zwicky (1933) Die Rotverschiebung von extragalaktischen Nebeln, Helvetica Physica Acta, 6, 110–127.

Galloway, G.J,, Khuri M.A. and Woolgar E. (2022) The topology of general cosmological models, IOP publishing. Classical Quantum Gravity **39** (2022) 195004 (14pp), https://doi.org/10.1088/1361-6382/ac75e1.

Guth, Alan H.; Tye, S.H. H. (1980) "Phase Transitions and Magnetic Monopole Production in the Very Early Universe". Phys. Rev. Lett. 44 (10): 631–635. Bibcode:1980PhRvL..44..631G. doi:10.1103/PhysRevLett.44.631. OSTI 1447535.

https://www.researchgate.net/publication/312597039_Extremal_Subsystems_of_Monotonic_Systems_I-II_Revised_2024 ; (2022) c) Monotone Phenomena of Issues Behind Bargaining Games and Data Analysis, https://www.mijnbestseller.nl/books/301785, ISBN 9789403645445,

Kibble, T. W. B. (1980) "Some implications of a Cosmological Phase Transition". Phys. Rep. 67 (1): 183–199. Bibcode:1980PhR..67..183K. https://doi:10.1016/0370-1573(80)90091-5 .

Krasnov, K. (2011) Gravity as a diffeomorphism invariant gauge theory. Physical Review D, 84(2), 024034.

Landau, L.D. and Lifshitz, E.M. (1971) The classical theory of fields. 3rd rev. edn. Course of Theoretical Physics, vol. 2. USSR Academy of Sciences: Pergamon. (https://www.datalaundering.com/download/LandauLifshitz.pdf, 27.02.2025).

Mullat, J.E. (1971) a) Tallinna Polütehnilise Instituudi Toimetised, Труды Таллинского Политехнического Института, Очерки по оброботке информоции, Серия А, №313, 37-44, https://www.datalaundering.com/download/modular-inter.pdf, accessed, 29.04.2026; (1976,1977) b) Extremal subsystems of monotonic systems, I, II and III. Avtom. and Telem., I, 5, pp. 130-139; II, 8, pp. 169-177; and III, 1, pp. 109-119;

Putz, Mihai V. & Ori, Ottorino (2026) Lemmas on topological symmetry between toroidal and Klein bottle fullerenes, Fullerenes, Nanotubes and Carbon Nanostructures, 34:4, 329-335, https://doi:10.1080/1536383X.2025.2540011.

Rovelli, C. (2004) Quantum Gravity. Cambridge: Cambridge University Press; (2018) The Order of Time. London: Allen Lane.

Rubin, Vera and Ford, Kent (1970) a) Rotation of the Andromeda Nebula from a spectroscopic survey of emission regions, Astrophysical Journal, 159, 379; (1980) b) Vera Rubin, W. Kent Ford Jr. & Norbert Thonnard Rotational properties of 21 Sc galaxies with a large range of luminosities and radii, Astrophysical Journal, 238, 471–487.

Sklyarenko, E.G. (2008) Курс лекций по классической дифференциальной геометрии: Moscow State University, Department of Higher Geometry and Topology, p.32. (http://www.datalaundering.com/download/Sklyarenkokurs.pdf, accessed, 06.04.2025).

Witten, Edward (1984) ″Cosmic separation of phases″. Physical Review D. 30 (2): 272–285. Bibcode:1981NuPhB.177..477W. doi:10.1103/PhysRevD.30.272. ISSN 0556-2821.